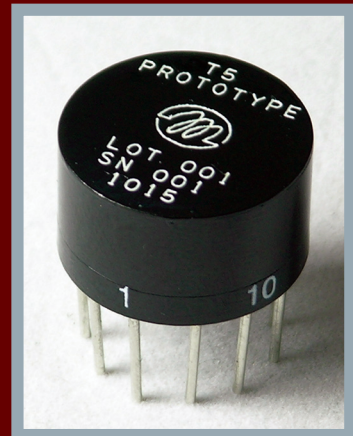
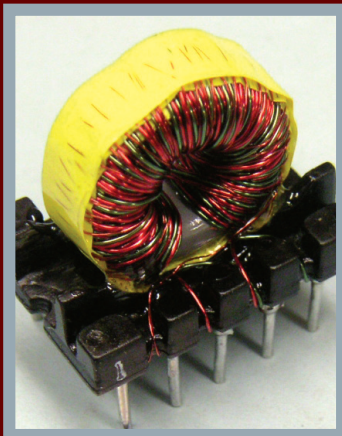
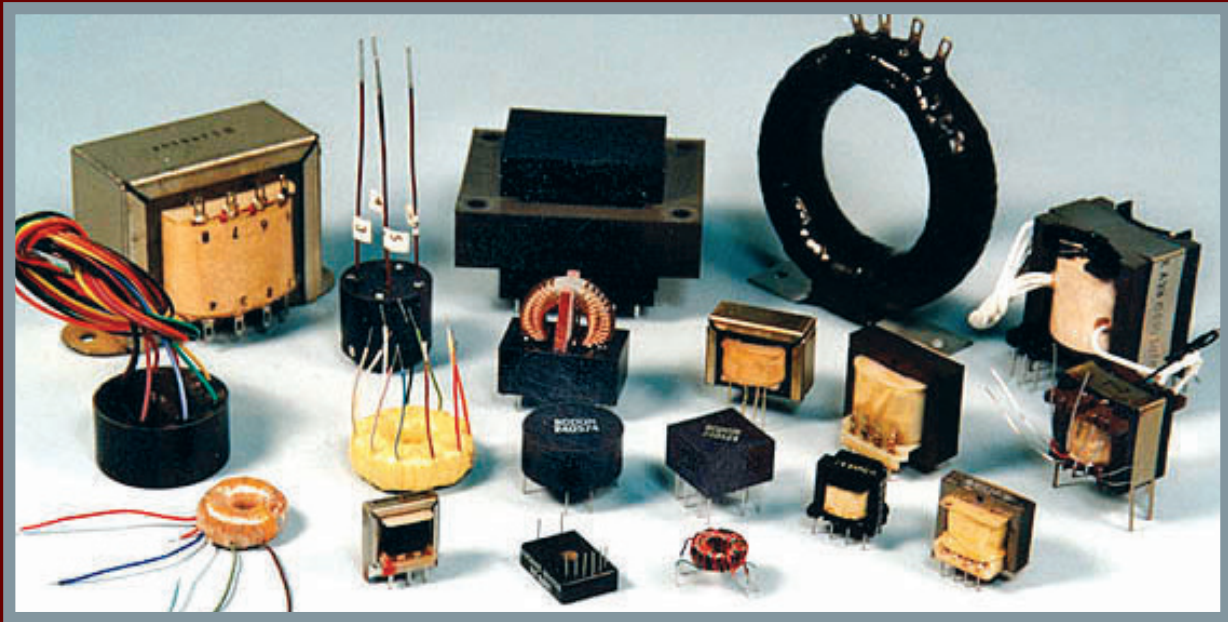


Transformer and Inductor Design Handbook

FOURTH EDITION



Colonel Wm. T. McLyman

Transformer and Inductor Design Handbook

FOURTH EDITION

Transformer and Inductor Design Handbook

FOURTH EDITION

Colonel Wm. T. McLyman



CRC Press
Taylor & Francis Group
Boca Raton London New York

CRC Press is an imprint of the
Taylor & Francis Group, an **informa** business

CRC Press
Taylor & Francis Group
6000 Broken Sound Parkway NW, Suite 300
Boca Raton, FL 33487-2742

© 2011 by Taylor & Francis Group, LLC
CRC Press is an imprint of Taylor & Francis Group, an Informa business

No claim to original U.S. Government works
Version Date: 2011907

International Standard Book Number-13: 978-1-4398-3688-0 (eBook - PDF)

This book contains information obtained from authentic and highly regarded sources. Reasonable efforts have been made to publish reliable data and information, but the author and publisher cannot assume responsibility for the validity of all materials or the consequences of their use. The authors and publishers have attempted to trace the copyright holders of all material reproduced in this publication and apologize to copyright holders if permission to publish in this form has not been obtained. If any copyright material has not been acknowledged please write and let us know so we may rectify in any future reprint.

Except as permitted under U.S. Copyright Law, no part of this book may be reprinted, reproduced, transmitted, or utilized in any form by any electronic, mechanical, or other means, now known or hereafter invented, including photocopying, microfilming, and recording, or in any information storage or retrieval system, without written permission from the publishers.

For permission to photocopy or use material electronically from this work, please access www.copyright.com (<http://www.copyright.com/>) or contact the Copyright Clearance Center, Inc. (CCC), 222 Rosewood Drive, Danvers, MA 01923, 978-750-8400. CCC is a not-for-profit organization that provides licenses and registration for a variety of users. For organizations that have been granted a photocopy license by the CCC, a separate system of payment has been arranged.

Trademark Notice: Product or corporate names may be trademarks or registered trademarks, and are used only for identification and explanation without intent to infringe.

Visit the Taylor & Francis Web site at
<http://www.taylorandfrancis.com>

and the CRC Press Web site at
<http://www.crcpress.com>

To My Wife, Bonnie

Contents

Foreword ix

Preface xi

Acknowledgements xiii

About the Author xv

Symbols xvii

Chapter 1

Fundamentals of Magnetics 1-1

Chapter 2

Magnetic Materials and Their Characteristics 2-1

Chapter 3

Magnetic Cores 3-1

Chapter 4

Window Utilization, Magnet Wire, and Insulation 4-1

Chapter 5

Transformer Design Trade-Offs 5-1

Chapter 6

Transformer-Inductor Efficiency, Regulation, and Temperature Rise 6-1

Chapter 7

Power Transformer Design 7-1

Chapter 8

DC Inductor Design, Using Gapped Cores 8-1

Chapter 9

DC Inductor Design, Using Powder Cores 9-1

Chapter 10

AC Inductor Design 10-1

Chapter 11

Constant Voltage Transformer (CVT) 11-1

Chapter 12

Three-Phase Transformer Design 12-1

	Chapter 13	
Flyback Converters, Transformer Design		13-1
	Chapter 14	
Forward Converter, Transformer Design, and Output Inductor Design		14-1
	Chapter 15	
Input Filter Design		15-1
	Chapter 16	
Current Transformer Design		16-1
	Chapter 17	
Winding Capacitance and Leakage Inductance		17-1
	Chapter 18	
Quiet Converter Design		18-1
	Chapter 19	
Rotary Transformer Design		19-1
	Chapter 20	
Planar Transformers and Inductors		20-1
	Chapter 21	
Derivations for the Design Equations		21-1
	Chapter 22	
Autotransformer Design		22-1
	Chapter 23	
Common-Mode Inductor Design		23-1
	Chapter 24	
Series Saturable Reactor Design		24-1
	Chapter 25	
Self-Saturating, Magnetic Amplifiers		25-1
	Chapter 26	
Designing Inductors for a Given Resistance		26-1

Foreword

Colonel McLyman is a well-known author, lecturer and magnetic circuit designer. His previous books on transformer and inductor design, magnetic core characteristics and design methods for converter circuits have been widely used by magnetics circuit designers.

In his 4th edition, Colonel McLyman has combined and updated the information found in his previous books. He has also added five new subjects such as autotransformer design, common-mode inductor design, series saturable reactor design, self-saturating magnetic amplifier and designing inductors for a given resistance. The author covers magnetic design theory with all of the relevant formulas. He has complete information on all of the magnetic materials and core characteristics along with the real world, step-by-step design examples.

This book is a must for engineers doing magnetic design. Whether you are working on high “rel” state of the art design or high volume, or low cost production, this book will help you. Thanks Colonel for a well-done, useful book.

*Robert G. Noah
Application Engineering Manager (Retired)
Magnetics, Division of Spang and Company
Pittsburgh, Pennsylvania*

Preface

I have had many requests to update my book *Transformer and Inductor Design Handbook*, because of the way power electronics has changed in the past few years. I have been requested to add and expand on the present Chapters. There are now twenty-six Chapters. The new Chapters are autotransformer design, common-mode inductor design, series saturable reactor design, self-saturating magnetic amplifier and designing inductors for a given resistance, all with step-by-step design examples.

This book offers a practical approach with design examples for design engineers and system engineers in the electronics industry, as well as the aerospace industry. While there are other books available on electronic transformers, none of them seem to have been written with the user's viewpoint in mind. The material in this book is organized so that the design engineer, student engineer or technician, starting at the beginning of the book and continuing through the end, will gain a comprehensive knowledge of the state of the art in transformer and inductor design. The more experienced engineers and system engineers will find this book a useful tool when designing or evaluating transformers and inductors.

Transformers are to be found in virtually all electronic circuits. This book can easily be used to design light-weight, high-frequency aerospace transformers or low-frequency commercial transformers. It is, therefore, a design manual.

The conversion process in power electronics requires the use of transformers, components that frequently are the heaviest and bulkiest item in the conversion circuit. Transformer components also have a significant effect on the overall performance and efficiency of the system. Accordingly, the design of such transformers has an important influence on overall system weight, power conversion efficiency, and cost. Because of the interdependence and interaction of these parameters, judicious trade-offs are necessary to achieve design optimization.

Manufacturers have for years assigned numeric codes to their cores to indicate their power-handling ability. This method assigns to each core a number called the area product, A_p , that is the product of its window area, W_a , and core cross-section area, A_c . These numbers are used by core suppliers to summarize dimensional and electrical properties in their catalogs. The product of the window area, W_a , and the core area, A_c , gives the area product, A_p , a dimension to the fourth power. I have developed a new equation for the power-handling ability of the core, the core geometry, K_g . The core geometry, K_g , has a dimension to the fifth power. This new equation gives engineers faster and tighter control of their design. The core geometry coefficient, K_g , is a relatively new concept, and magnetic core manufacturers are now beginning to put it in their catalogs.

Because of their significance, the area product, A_p , and the core geometry, K_g , are treated extensively in this handbook. A great deal of other information is also presented for the convenience of the designer. Much of the material is in tabular form to assist the designer in making the trade-offs best suited for the particular application in a minimum amount of time.

Designers have used various approaches in arriving at suitable transformer and inductor designs. For example, in many cases a rule of thumb used for dealing with current density is that a good working level is 1000 circular mils per ampere. This is satisfactory in many instances; however, the wire size used to meet this requirement may produce a heavier and bulkier inductor than desired or required. The information presented here will make it possible to avoid the use of this and other rules of thumb, and to develop a more economical and better design.

The author or the publisher assumes no responsibility for any infringement of patent or other rights of third parties that may result from the use of circuits, systems, or processes described or referred to in this handbook.

I wish to thank the manufacturers represented in this book for their assistance in supplying technical data.

Colonel Wm. T. McLyman

Acknowledgements

In gathering the material for this book, I have been fortunate in having the assistance and cooperation of several companies and many colleagues. As the author, I wish to express my gratitude to all of them. The list is too long to mention them all. However, there are some individuals and companies whose contributions have been significant. Colleagues that have retired from Magnetics include Robert Noah and Harry Savisky who helped so greatly with the editing of the final draft. Other contributions were given by my colleagues at Magnetics, Lowell Bosley and his staff with the sending of up-to-date catalogs and sample cores. I would like to thank colleagues at Micrometals Corp., Jim Cox and Dale Nicol, and George Orenchak of TSC International. I would like to give a special thanks to Richard (Oz) Ozenbaugh of Linear Magnetics Corp. for his assistance in the detailed derivations of many of the equations and his efforts in checking all the design examples. I would also like to give special thanks to Steve Freeman of Rodon Products, Inc. and Charles Barnett of Leightner Electronics, Inc. for building and testing all of the magnetic components used in the design examples.

There are individuals I would like to thank: Dr. Vatche Vorperian of Jet Propulsion Laboratory (JPL) for his help in generating and clarifying equations for the Quiet Converter; Jerry Fridenberg of Fridenberg Research, Inc. for modeling circuits on his SPICE program; Dr. Gene Wester of (JPL) for his inputs and Kit Sum for his assistance in the energy storage equations. I also want to thank the late Robert Yahiro for his help and encouragement over the years.

About The Author

Colonel Wm. T. McLyman has retired as a senior member of the Avionics Equipment Section of the Jet Propulsion Laboratory (JPL) affiliated with the California Institute of Technology in Pasadena, California. He has fifty-four years of experience in the field of Magnetics and holds fourteen United States Patents on magnetics-related concepts. Through his thirty years at JPL, he has written over seventy JPL technical memorandums, new technology reports, and tech-briefs on the subject of magnetics and circuit designs for power conversion. He has worked on projects for NASA including the Pathfinder Mission to Mars, Cassini, Galileo, Magellan, Viking, Voyager, MVM, Hubble Space Telescope, and many others.

He has been on the lecture circuit for over twenty-nine years speaking in the United States, Canada, Mexico, and Europe on the design and fabrication of magnetic components. He is known as a recognized authority in magnetic design. He is the president of his company called Kg Magnetics, Inc., which specializes in power magnetics design.

He has also written a book entitled *Design and Fabrication of High Reliability Magnetic Devices*. This book is based on fabricating and testing Hi-Rel magnetic devices. He also markets through Kg Magnetics, Inc. a magnetics design and analysis software computer program called “Titan” for transformers and inductors, see Figure 1. This program operates on Windows 95, 98, 2000, and NT.

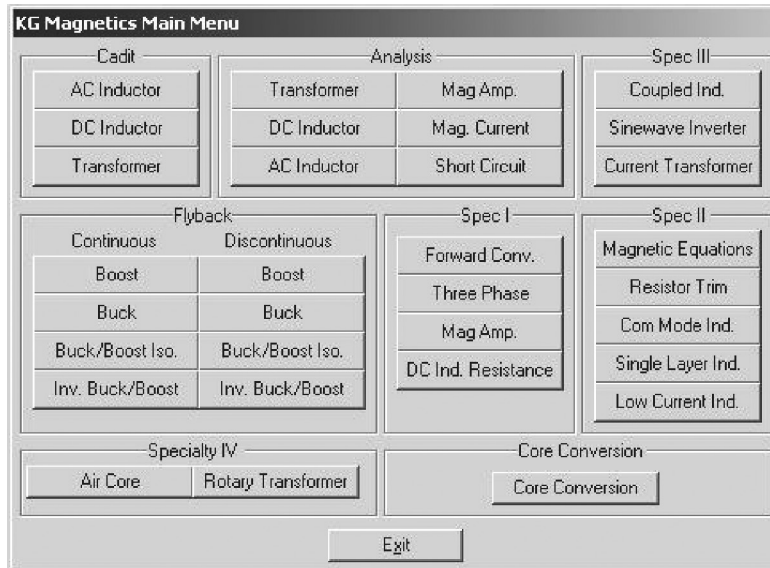


Figure 1. Computer Design Program Main Menu.

Kg Magnetics, Inc.
Colonel Wm. T. McLyman, (President)
www.kgmagnetics.com
colonel@kgmagnetics.com
Idyllwild, CA 92549

Symbols

α	regulation, %
A_c	effective cross section of the core, cm ²
A_p	area product, cm ⁴
A_t	surface area of the transformer, cm ²
A_w	wire area, cm ²
$A_{w(B)}$	bare wire area, cm ²
$A_{w(I)}$	insulated wire area, cm ²
A_{wp}	primary wire area, cm ²
A_{ws}	secondary wire area, cm ²
A-T	amp turn
AWG	American wire gage
B	flux, teslas
B_{ac}	alternating current flux density, teslas
ΔB	change in flux, teslas
B_{dc}	direct current flux density, teslas
B_m	flux density, teslas
B_{max}	maximum flux density, teslas
B_o	operating peak flux density, teslas
B_{pk}	peak flux density, teslas
B_r	residual flux density, teslas
B_s	saturation flux density, teslas
C	capacitance
C_n	new capacitance
C_p	lumped capacitance
C_s	stray capacitance
CM	circular mils
CM	common mode
D_{AWG}	wire diameter, cm
$D_{(min)}$	minimum duty ratio
$D_{(max)}$	maximum duty ratio
D_w	dwell time duty ratio
DM	differential mode
E	voltage
E_{Line}	line-to-line voltage
E_{Phase}	Line to neutral voltage
Energy	energy, watt-second
ESR	equivalent series resistance

η	efficiency
f	frequency, Hz
F	fringing flux factor
F_m	magneto-motive force, mmf
F.L.	full load
G	winding length, cm
γ	density, in grams-per-cm ²
ϵ	skin depth, cm
H	magnetizing force, oersteds
H	magnetizing force, amp-turns
H_c	magnetizing force required to return flux to zero, oersteds
ΔH	delta magnetizing force, oersteds
H_o	operating peak magnetizing force
H_s	magnetizing force at saturation, oersteds
I	current, amps
I_c	charge current, amps
I_c	control current, amps
ΔI	delta current, amps
I_{dc}	dc current, amps
I_g	gate current, amps
I_{in}	input current, amps
I_{Line}	input line current, amps
I_m	magnetizing current, amps
I_o	load current, amps
$I_{o(max)}$	maximum load current, amps
$I_{o(min)}$	minimum load current, amps
I_p	primary current, amps
I_{Phase}	input phase current, amps
I_s	secondary current, amps
$I_{s(Phase)}$	secondary phase current, amps
$I_{s(Line)}$	secondary line current, amps
J	current density, amps per cm ²
K_c	copper loss constant
K_c	quasi-voltage waveform factor
K_e	electrical coefficient
K_{cw}	control winding coefficient
K_f	waveform coefficient

K_g	core geometry coefficient, cm^5
K_j	constant related to current density
K_s	constant related to surface area
K_u	window utilization factor
K_{up}	primary window utilization factor
K_{us}	secondary window utilization factor
K_{vol}	constant related to volume
K_w	constant related to weight
L	inductance, henry
l	is a linear dimension
λ	density, grams per cm^3
L_c	open circuit inductance, henrys
L_c	control winding inductance, henrys
$L_{(crt)}$	critical inductance
l_g	gap, cm
l_m	magnetic path length, cm
L_p	primary inductance, henrys
l_t	total path length, cm
MA	magnetic amplifier
mks	meters-kilogram-seconds
MLT	mean length turn, cm
mmf	magnetomotive force, F_m
MPL	magnetic path length, cm
mW/g	milliwatts-per-gram
μ	permeability
μ_e	effective permeability
μ_i	initial permeability
μ_Δ	incremental permeability
μ_m	core material permeability
μ_o	permeability of air
μ_r	relative permeability
n	turns ratio
N	turns
N_c	control turns
N_g	gate turns
N_L	inductor turns
N_n	new turns

xx**Symbols**

N_p	primary turns
N_s	secondary turns
N.L.	no load
P	watts
P_c	control power loss, watts
P_{cu}	copper loss, watts
P_{fe}	core loss, watts
P_g	gap loss, watts
P_{gain}	power gain, factor
ϕ	magnetic flux
P_{in}	input power, watts
P_L	inductor copper loss, watts
P_o	output power, watts
P_p	primary copper loss, watts
P_s	secondary copper loss, watts
P_{Σ}	total loss (core and copper), watts
P_t	total apparent power, watts
P_{tin}	autotransformer input power, volt-amps
P_{to}	autotransformer output power, volt-amps
P_{VA}	primary, volt-amps
R	resistance, ohms
R_{ac}	ac resistance, ohms
R_c	control resistance, ohms
R_{cu}	copper resistance, ohms
R_{dc}	dc resistance, ohms
R_e	equivalent core loss (shunt) resistance, ohms
R_g	reluctance of the gap
$R_{in(equiv)}$	reflected load resistance, ohms
R_L	load resistance, ohms
R_m	reluctance
R_{mt}	total reluctance
R_o	load resistance, ohms
$R_{o(R)}$	reflected load resistance, ohms
R_p	primary resistance, ohms
R_R	ac/dc resistance ratio
R_s	secondary resistance, ohms
R_t	total resistance, ohms

ρ	resistivity, ohm-cm
S_1	conductor area/wire area
S_2	wound area/usable window
S_3	usable window area/window area
S_4	usable window area/usable window area + insulation area
S_{np}	number of primary strands
S_{ns}	number of secondary strands
S_{VA}	secondary volt-amps
SR	saturable reactor
T	total period, seconds
t_{off}	off time, seconds
t_{on}	on time, seconds
t_r	time constant, seconds
T_r	temperature rise, degrees C
t_w	dwel time, seconds
U	multiplication factor
V_{ac}	applied voltage, volts
V_c	control voltage, volts
$V_{c(pk)}$	peak voltage, volts
V_d	diode voltage drop, volts
V_{in}	input voltage, volts
$V_{in(max)}$	maximum input voltage, volts
$V_{in(min)}$	minimum input voltage, volts
V_n	new voltage, volts
V_o	output voltage, volts
V_p	primary voltage, volts
$V_{p(rms)}$	primary rms voltage, volts
$V_{r(pk)}$	peak ripple voltage
$V_{s(LL)}$	secondary line-to-line voltage, volts
$V_{s(LN)}$	secondary line to neutral voltage, volts
V_s	secondary voltage, volts
ΔV_{CC}	capacitor voltage, volts
ΔV_{CR}	capacitor ESR voltage, volts
ΔV_p	delta primary voltage, volts
ΔV_s	delta secondary voltage, volts
VA	volt-amps
W	watts

W/kg	watts-per-kilogram
WK	watts-per-kilogram
W_a	window area, cm^2
W_{ac}	control window area, cm^2
$W_{a(eff)}$	effective window area, cm^2
W_{ag}	gate window area, cm^2
W_{ap}	primary window area, cm^2
W_{as}	secondary window area, cm^2
W_t	weight, grams
W_{tcu}	copper weight, grams
W_{tfe}	iron weight, grams
$w-s$	watt-seconds
X_L	inductive reactance, ohms

Chapter 1

Fundamentals of Magnetics

Table of Contents

1. Introduction.....	1-3
2. Magnetic Properties in Free Space	1-3
3. Intensifying the Magnetic Field	1-4
4. Simple Transformer	1-7
5. Magnetic Core.....	1-8
6. Fundamental Characteristics of a Magnetic Core	1-9
7. Hysteresis Loop (B-H Loop)	1-11
8. Permeability	1-12
9. Magnetomotive Force (mmf) and Magnetizing Force (H).....	1-15
10. Reluctance	1-16
11. Air Gap	1-18
12. Controlling the dc Flux with an Air Gap	1-20
13. Types of Air Gaps	1-21
14. Fringing Flux	1-22
15. Material Permeability, (μ_m).....	1-23
16. Air Gaps.....	1-23
17. Fringing Flux, F.....	1-24
18. Gapped, dc Inductor Design.....	1-25
19. Fringing Flux and Coil Proximity	1-26
20. Fringing Flux, Crowding	1-27
21. Fringing Flux and Powder Cores	1-28

Introduction

Considerable difficulty is encountered in mastering the field of magnetics because of the use of so many different systems of units – the centimeter-gram-second (cgs) system, the meter-kilogram-second (mks) system, and the mixed English units system. Magnetics can be treated in a simple way by using the cgs system. There always seems to be one exception to every rule and that is permeability.

Magnetic Properties in Free Space

A long wire with a dc current, I , flowing through it, produces a circulatory magnetizing force, H , and a magnetic field, B , around the conductor, as shown in Figure 1-1, where the relationship is:

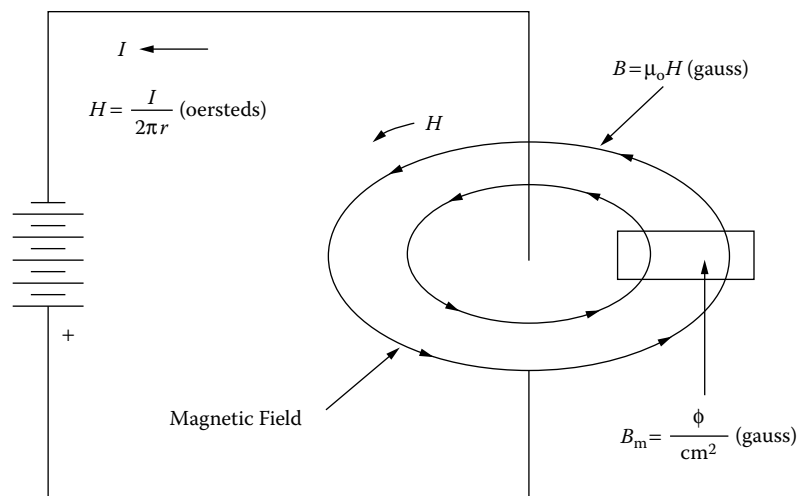


Figure 1-1. A Magnetic Field Generated by a Current Carrying Conductor.

The direction of the line of flux around a straight conductor may be determined by using the “right hand rule” as follows: When the conductor is grasped with the right hand, so that the thumb points in the direction of the current flow, the fingers point in the direction of the magnetic lines of force. This is based on so-called conventional current flow, not the electron flow.

When a current is passed through the wire in one direction, as shown in Figure 1-2(A), the needle in the compass will point in one direction. When the current in the wire is reversed, as in Figure 1-2(B), the needle will also reverse direction. This shows that the magnetic field has polarity and that, when the current I , is reversed, the magnetizing force, H , will follow the current reversals.

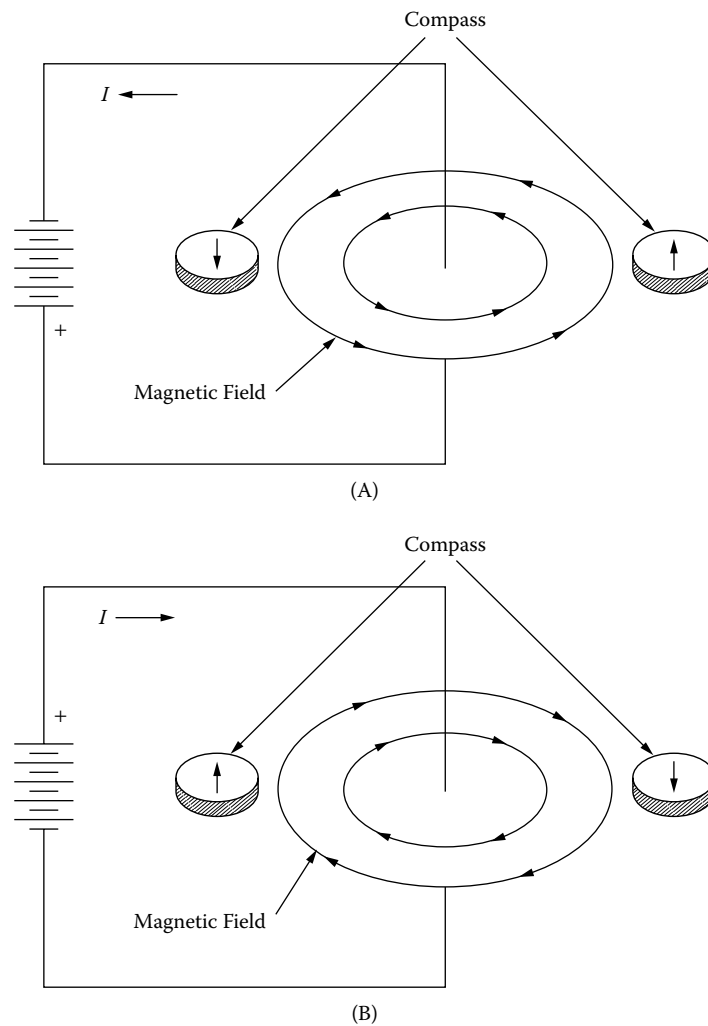


Figure 1-2. The Compass Illustrates How the Magnetic Field Changes Polarity.

Intensifying the Magnetic Field

When a current passes through a wire, a magnetic field is set up around the wire. If the conductors, as shown in Figure 1-3, carrying current in the same direction are separated by a relatively large distance, the magnetic fields generated will not influence each other. If the same two conductors are placed close to each other, as shown in Figure 1-4, the magnetic fields add, and the field intensity doubles.

$$\gamma = \frac{B^2}{8\pi\mu}, \quad [\text{energy density}] \quad [1-1]$$

If the wire is wound on a dowel, its magnetic field is greatly intensified. The coil, in fact, exhibits a magnetic field exactly like that of a bar magnet, as shown in Figure 1-5. Like the bar magnet, the coil has a north pole and a neutral center region. Moreover, the polarity can be reversed by reversing the current, I , through the coil. Again, this demonstrates the dependence of the magnetic field on the current direction.

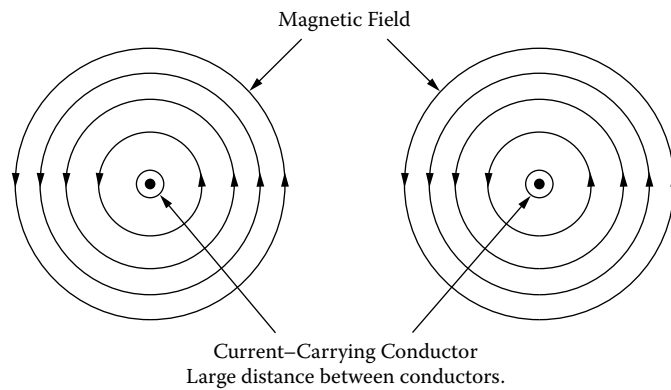


Figure 1-3. Magnetic Fields Produced Around Spaced Conductors.

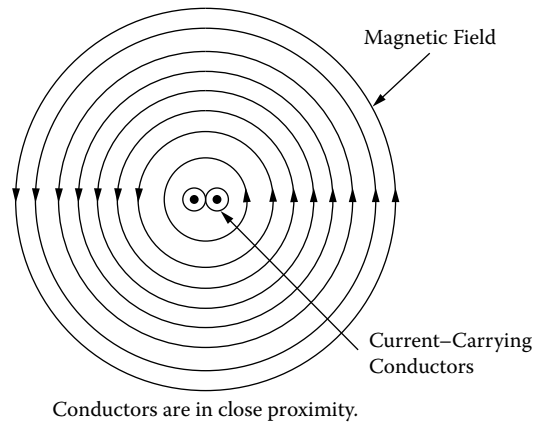


Figure 1-4. Magnetic Fields Produced Around Adjacent Conductors.

The magnetic circuit is the space in which the flux travels around the coil. The magnitude of the flux is determined by the product of the current, I , and the number of turns, N , in the coil. The force, NI , required to create the flux is magnetomotive force (mmf). The relationship between flux density, B , and magnetizing force, H , for an air-core coil is shown in Figure 1-6. The ratio of B to H is called the permeability, μ , and for this air-core coil the ratio is unity in the cgs system, where it is expressed in units of gauss per oersteds, (gauss/oersteds).

$$\mu_o = 1$$

$$B = \mu_o H \tag{1-2}$$

If the battery, in Figure 1-5, were replaced with an ac source, as shown in Figure 1-7, the relationship between B and H would have the characteristics shown in Figure 1-8. The linearity of the relationship between B and H represents the main advantage of air-core coils. Since the relationship is linear, increasing H increases B , and therefore the flux in the coil, and, in this way, very large fields can be produced with large currents. There is obviously a practical limit to this, which depends on the maximum allowable current in the conductor and the resulting rise.

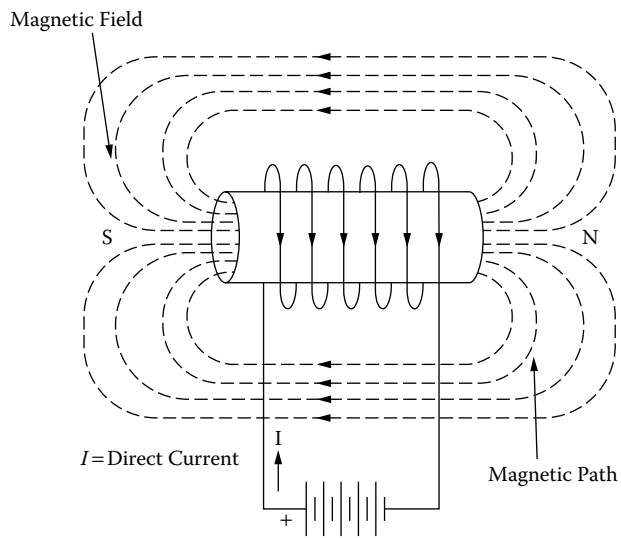


Figure 1-5. Air-Core Coil with dc Excitation.

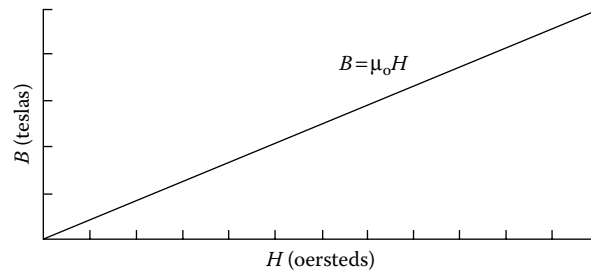


Figure 1-6. Relationship between B and H with dc Excitation.

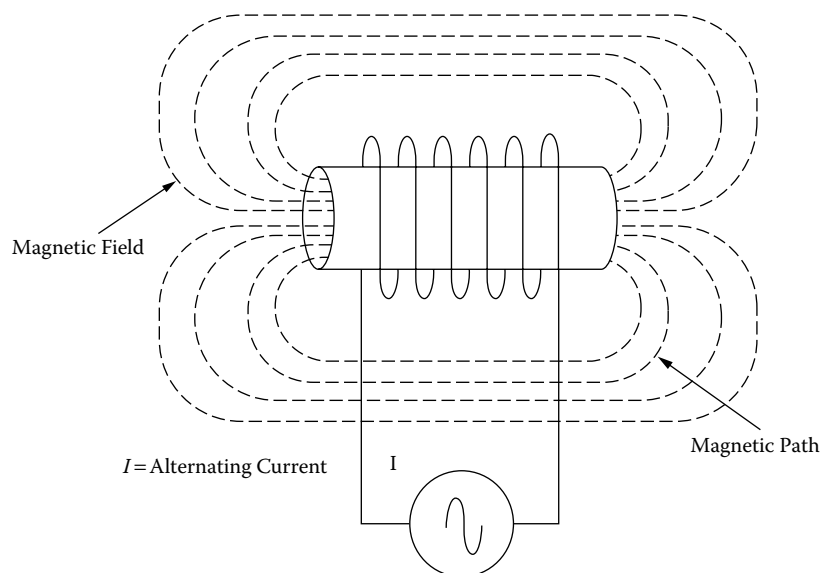


Figure 1-7. Air-Core Coil Driven from an ac Source.

Fields of the order of 0.1 tesla are feasible for a 40°C temperature rise above room ambient temperature. With super cooled coils, fields of 10 tesla have been obtained.

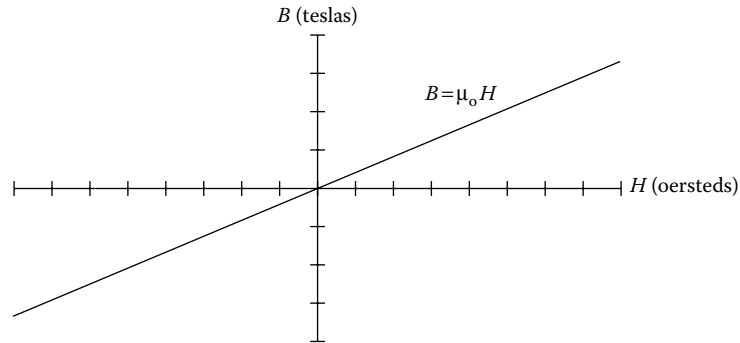


Figure 1-8. Relationship between B and H with ac Excitation.

Simple Transformer

A transformer in its simplest form is shown in Figure 1-9. This transformer has two air coils that share a common flux. The flux diverges from the ends of the primary coil in all directions. It is not concentrated or confined. The primary is connected to the source and carries the current that establishes a magnetic field. The other coil is open-circuited. Notice that the flux lines are not common to both coils. The difference between the two is the leakage flux; that is, leakage flux is the portion of the flux that does not link both coils.

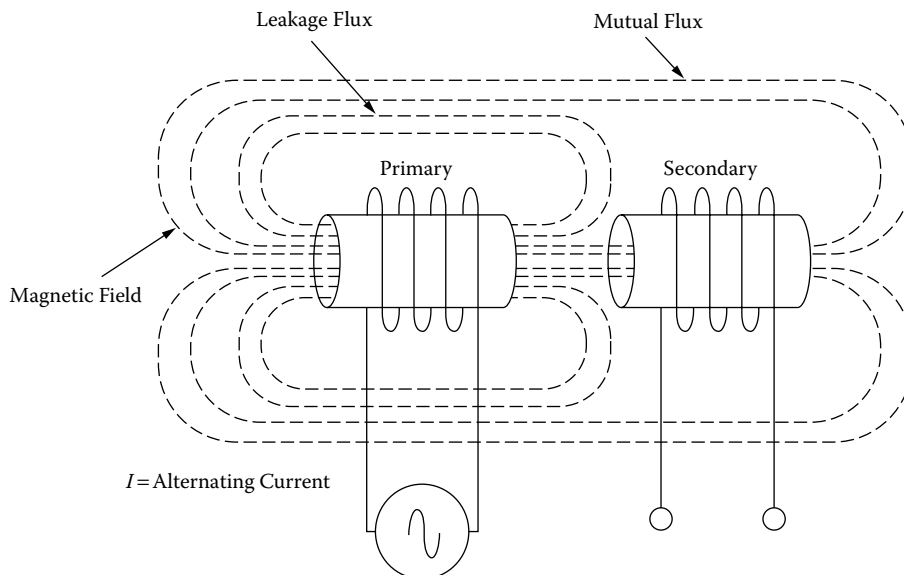


Figure 1-9. The Simplest Type of Transformer.

Magnetic Core

Most materials are poor conductors of magnetic flux; they have low permeability. A vacuum has a permeability of 1.0, and nonmagnetic materials, such as air, paper, and copper have permeabilities of the same order. There are a few materials, such as iron, nickel, cobalt, and their alloys that have high permeability, sometimes ranging into the hundreds of thousands. To achieve an improvement over the air-coil, as shown in Figure 1-10, a magnetic core can be introduced, as shown in Figure 1-11. In addition to its high permeability, the advantages of the magnetic core over the air-core are that the Magnetic Path Length (MPL) is well-defined, and the flux is essentially confined to the core, except in the immediate vicinity of the winding. There is a limit as to how much magnetic flux can be generated in a magnetic material before the magnetic core goes into saturation, and the coil reverts back to an air-core, as shown in Figure 1-12.

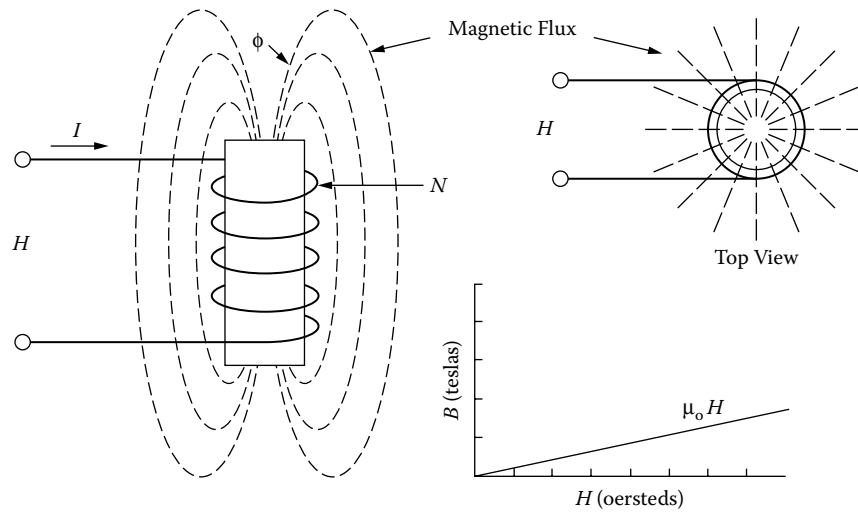


Figure 1-10. Air-Core Coil Emitting Magnetic Flux when Excited.

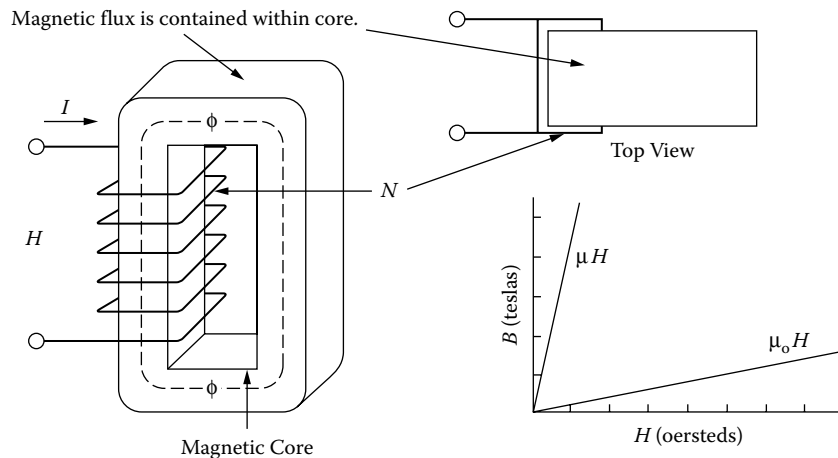


Figure 1-11. Introduction of a Magnetic Core.

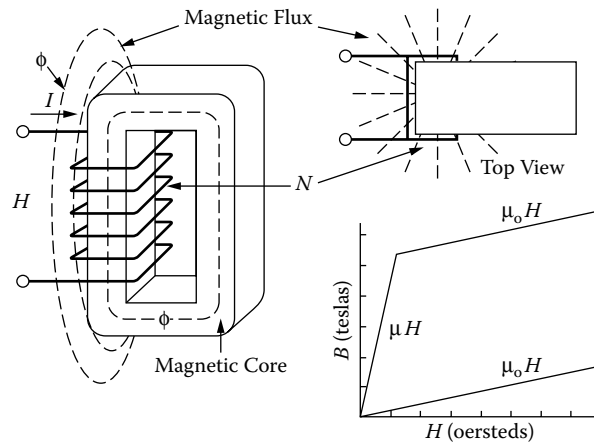


Figure 1-12. Excited Magnetic Core Driven into Saturation.

Fundamental Characteristics of a Magnetic Core

The effect of exciting a completely demagnetized, ferromagnetic material, with an external magnetizing force, \$H\$, and increasing it slowly, from zero, is shown in Figure 1-13, where the resulting flux density is plotted as a function of the magnetizing force, \$H\$. Note that, at first, the flux density increases very slowly up to point A, then, increases very rapidly up to point B, and then, almost stops increasing. Point B is called the knee of the curve. At point C, the magnetic core material has saturated. From this point on, the slope of the curve is shown in Equation [1-3].

$$\frac{B}{H} = 1, \text{ [gauss/oersteds]} \tag{1-3}$$

The coil is now behaving as if it had an air-core. When the magnetic core is in hard saturation, the coil has the same permeability as air, or unity. Following the magnetization curve in Figure 1-14, Figures 1-15 through Figures 1-16 show how the flux in the core is generated from the inside of the core to the outside until the core saturates.

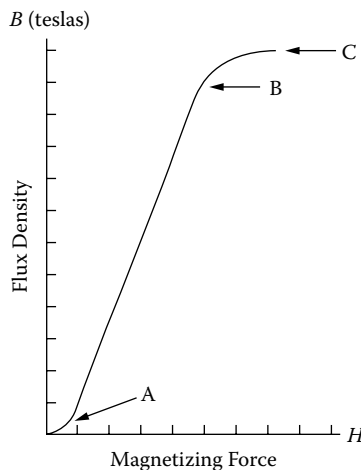


Figure 1-13. Typical Magnetization Curve.

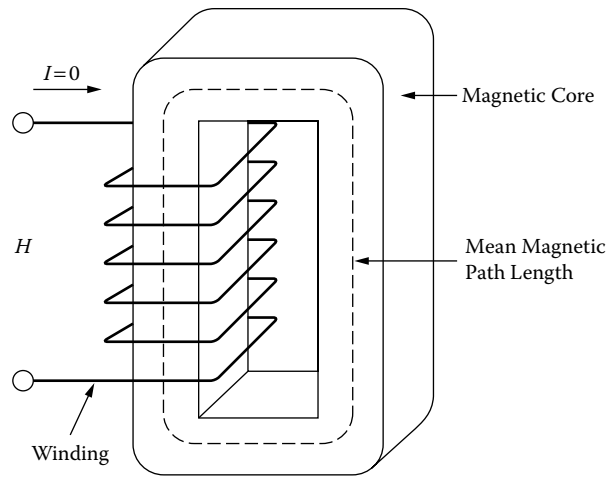


Figure 1-14. Magnetic Core with Zero Excitation.

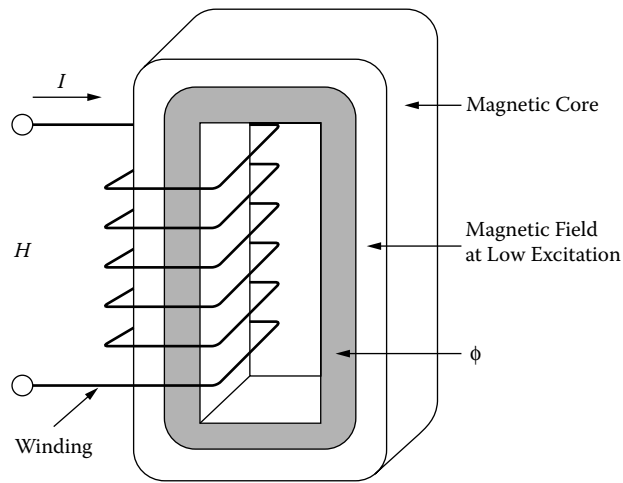


Figure 1-15. Magnetic Core with Low Excitation.

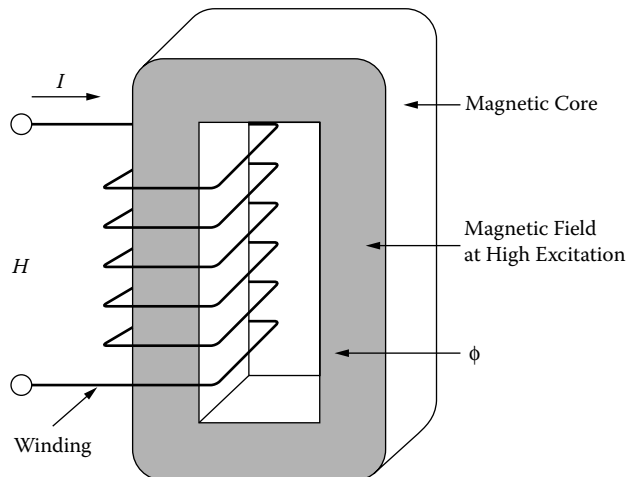


Figure 1-16. Magnetic Core with High Excitation.

Hysteresis Loop (B-H Loop)

An engineer can take a good look at the hysteresis loop and get a first order evaluation of the magnetic material. When the magnetic material is taken through a complete cycle of magnetization and demagnetization, the results are as shown in Figure 1-17. It starts with a neutral magnetic material, traversing the B-H loop at the origin X. As H is increased, the flux density B increases along the dashed line to the saturation point, B_s . When H is now decreased and B is plotted, B-H loop transverses a path to B_r , where H is zero and the core is still magnetized. The flux at this point is called remanent flux, and has a flux density, B_r .

The magnetizing force, H, is now reversed in polarity to give a negative value. The magnetizing force required to reduce the flux B_r to zero is called the coercive force, H_c . When the core is forced into saturation, the retentivity, B_{rs} , is the remaining flux after saturation, and coercivity, H_{cs} , is the magnetizing force required to reset to zero. Along the initial magnetization curve at point X, the dashed line in Figure 1-17, B increases from the origin nonlinearly with H, until the material saturates. In practice, the magnetization of a core in an excited transformer never follows this curve, because the core is never in the totally demagnetized state, when the magnetizing force is first applied.

The hysteresis loop represents energy lost in the core. The best way to display the hysteresis loop is to use a dc current, because the intensity of the magnetizing force must be so slowly changed so that no eddy currents are generated in the material. Only under this condition is the area inside the closed B-H loop indicative of the hysteresis. The enclosed area is a measure of energy lost in the core material during that cycle. In ac applications, this process is repeated continuously and the total hysteresis loss is dependent upon the frequency.

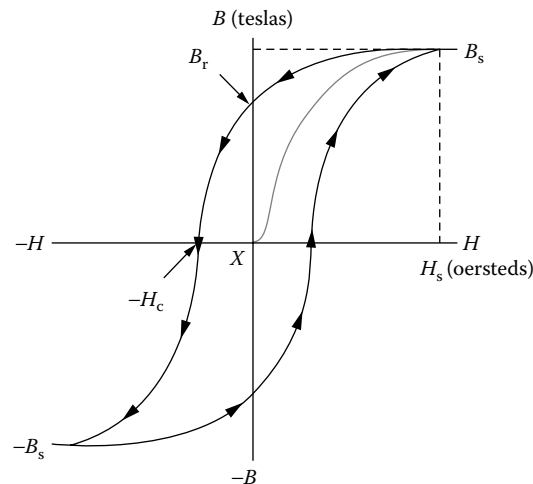


Figure 1-17. Typical Hysteresis Loop.

Permeability

In magnetics, permeability is the ability of a material to conduct flux. The magnitude of the permeability at a given induction is the measure of the ease with which a core material can be magnetized to that induction. It is defined as the ratio of the flux density, B, to the magnetizing force, H. Manufacturers specify permeability in units of gauss per oersteds, as shown in Equation [1-4].

$$\text{Permeability} = \frac{B}{H}, \left[\frac{\text{gauss}}{\text{oersteds}} \right] \quad [1-4]$$

The absolute permeability, μ_o in cgs units is unity 1 (gauss per oersteds) in a vacuum, as shown in Equation [1-5].

$$\text{cgs: } \mu_o = 1, \left[\frac{\text{gauss}}{\text{oersteds}} \right] = \left[\frac{\text{teslas}}{\text{oersteds}} (10^4) \right] \quad [1-5]$$

$$\text{mks: } \mu_o = 0.4\pi(10^{-8}), \left[\frac{\text{henrys}}{\text{meter}} \right]$$

When B is plotted against H, as in Figure 1-18, the resulting curve is called the magnetization curve. These curves are idealized. The magnetic material is totally demagnetized and is then subjected to gradually increasing magnetizing force, while the flux density is plotted. The slope of this curve at any given point gives the permeability at that point. Permeability can be plotted against a typical B-H curve, as shown in Figure 1-19. Permeability is not constant; therefore, its value can be stated only at a given value of B or H.

There are many different kinds of permeability, and each is designated by a different subscript on the symbol μ .

- μ_o 1. Absolute permeability, defined as the permeability in a vacuum.
- μ_i 2. Initial permeability is the slope of the initial magnetization curve at the origin. It is measured at very small induction, as shown in Figure 1-20.
- μ_Δ 3. Incremental permeability is the slope of the magnetization curve for finite values of peak-to-peak flux density with superimposed dc magnetization, as shown in Figure 1-21.
- μ_e 4. Effective permeability. If a magnetic circuit is not homogeneous (i.e., contains an air gap), the effective permeability is the permeability of hypothetical homogeneous (ungapped) structure of the same shape, dimensions, and reluctance that would give the inductance equivalent to the gapped structure.
- μ_r 5. Relative permeability is the permeability of a material relative to that of free space.
- μ_n 6. Normal permeability is the ratio of B/H at any point of the curve, as shown in Figure 1-22.
- μ_{\max} 7. Maximum permeability is the slope of a straight line drawn from the origin tangent to the curve at its knee, as shown in Figure 1-23.
- μ_p 8. Pulse permeability is the ratio of peak B to peak H for unipolar excitation.
- μ_m 9. Material permeability is the slope of the magnetization curve measure at less than 50 gauss, as shown in Figure 1-24.

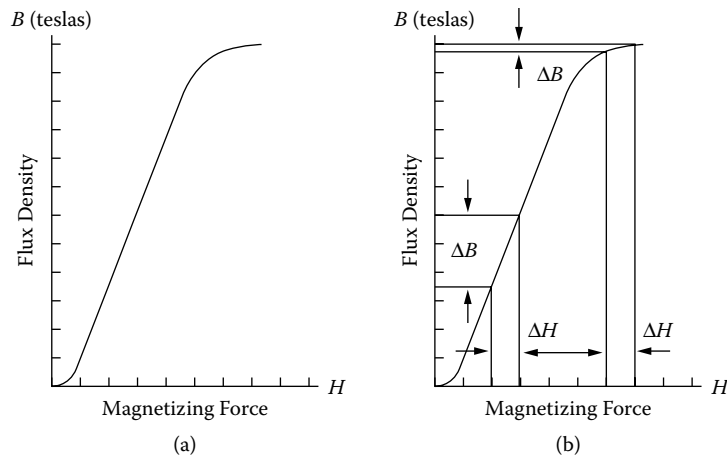


Figure 1-18. Magnetizing Curve.

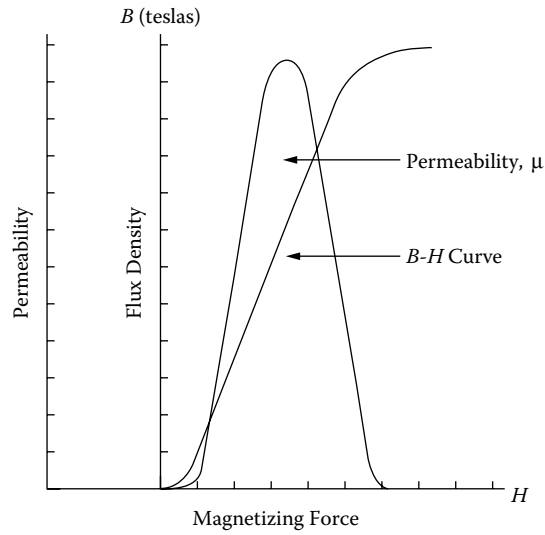


Figure 1-19. Variation of Permeability μ along the Magnetizing Curve.

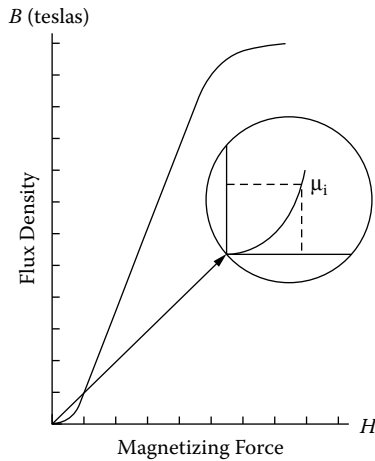


Figure 1-20. Initial Permeability.

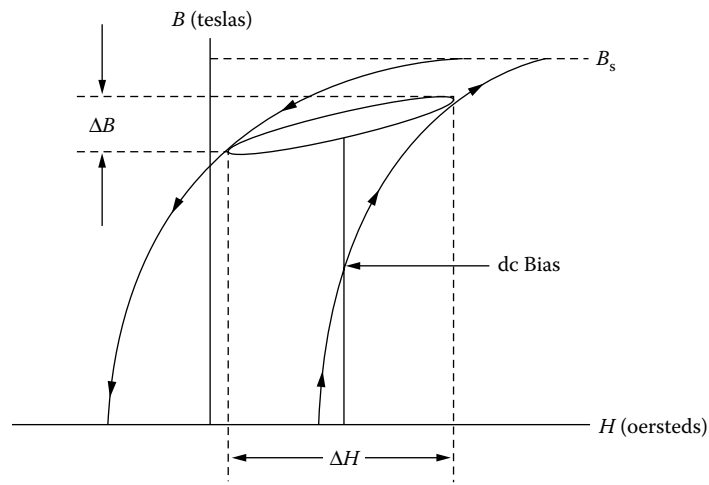


Figure 1-21. Incremental Permeability.

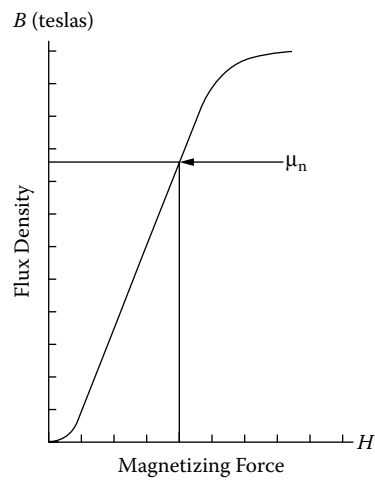


Figure 1-22. Normal Permeability.

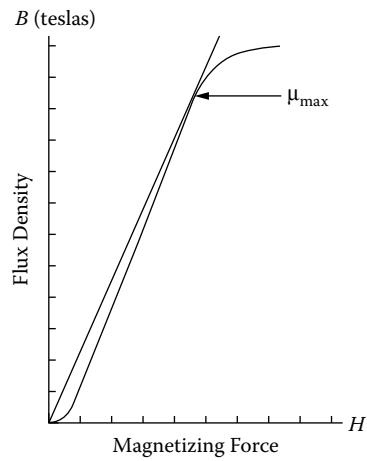


Figure 1-23. Maximum Permeability.

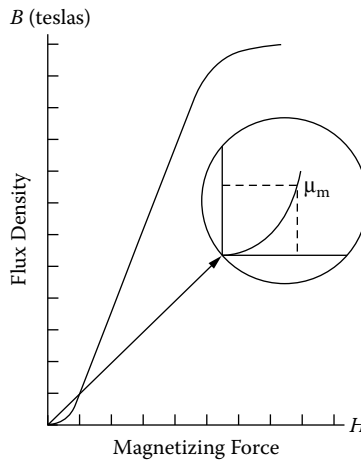


Figure 1-24. Material Permeability.

Magnetomotive Force (mmf) and Magnetizing Force (H)

There are two force functions commonly encountered in magnetics: magnetomotive force, mmf, and magnetizing force, H. Magnetomotive force should not be confused with magnetizing force; the two are related as cause and effect. Magnetomotive force is given by the Equation [1-6].

$$\text{mmf} = 0.4\pi NI, \quad [\text{gilberts}] \tag{1-6}$$

N is the number of turns and I is the current in amperes. Whereas mmf is the force, H is a force field, or force per unit length, as shown in Equation [1-7].

$$H = \frac{\text{mmf}}{\text{MPL}}, \quad \left[\frac{\text{gilberts}}{\text{cm}} = \text{oersteds} \right] \tag{1-7}$$

Substituting,

$$H = \frac{0.4\pi NI}{\text{MPL}}, \quad [\text{oersteds}] \tag{1-8}$$

MPL = Magnetic Path Length in cm.

If the flux is divided by the core area, A_c , we get flux density, B, in lines per unit area, as shown in Equation [1-9].

$$B = \frac{\phi}{A_c}, \quad [\text{gauss}] \tag{1-9}$$

The flux density, B, in a magnetic medium, due to the existence of a magnetizing force H, depends on the permeability of the medium and the intensity of the magnetic field, as shown in Equation [1-10].

$$B = \mu H, \quad [\text{gauss}] \tag{1-10}$$

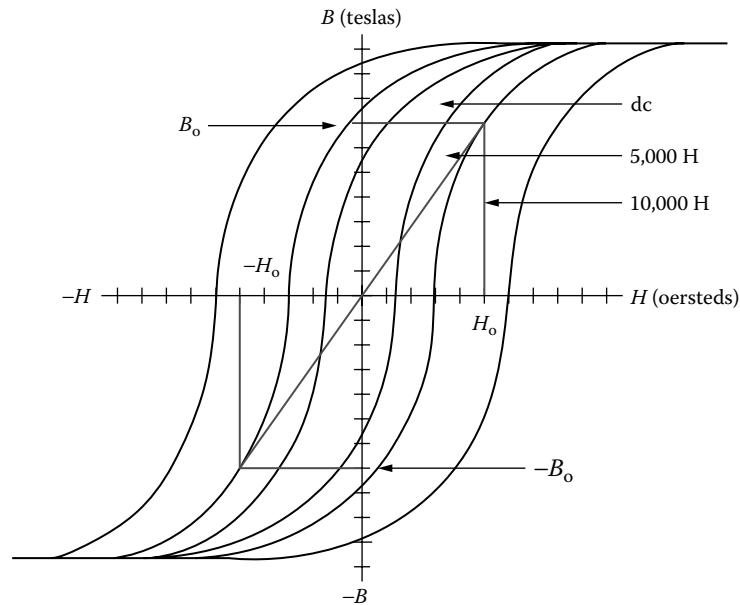


Figure 1-25. Typical B-H Loops Operating at Various Frequencies.

The peak magnetizing current, I_m , for a wound core can be calculated from the following Equation [1-11].

$$I_m = \frac{H_o(MPL)}{0.4\pi N}, \quad [\text{amps}] \quad [1-11]$$

H_o is the field intensity at the peak operating point. To determine the magnetizing force, H_o , use the manufacturer's core loss curves at the appropriate frequency and operating flux density, B_o , as shown in Figure 1-25.

Reluctance

The flux produced in a given material by magnetomotive force (mmf) depends on the material's resistance to flux, which is called reluctance, R_m . The reluctance of a core depends on the composition of the material and its physical dimension and is similar in concept to electrical resistance. The relationship between mmf, flux, and magnetic reluctance is analogous to the relationship between emf, current, and resistance, as shown in Figure 1-26.

$$\begin{aligned} \text{emf } (E) &= IR = \text{Current} \times \text{Resistance} \\ \text{mmf } (F_m) &= \Phi R_m = \text{Flux} \times \text{Reluctance} \end{aligned} \quad [1-12]$$

A poor conductor of flux has a high magnetic resistance, R_m . The greater the reluctance, the higher the magnetomotive force that is required to obtain a given magnetic field.

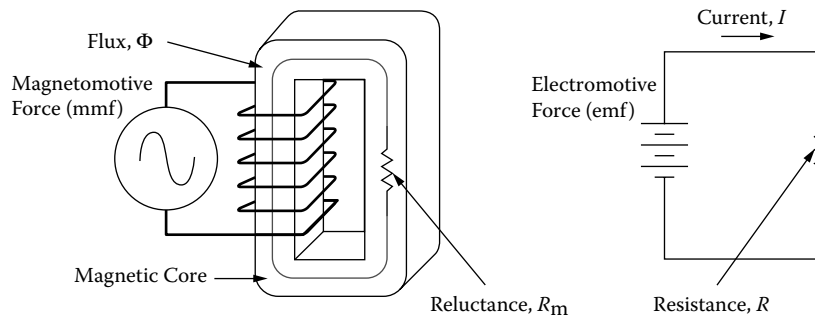


Figure 1-26. Comparing Magnetic Reluctance and Electrical Resistance.

The electrical resistance of a conductor is related to its length l , cross-sectional area A_w , and specific resistance ρ , which is the resistance per unit length. To find the resistance of a copper wire of any size or length, we merely multiply the resistivity by the length, and divide by the cross-sectional area, as shown in Equation [1-13].

$$R = \frac{\rho l}{A_w}, \quad [\text{ohms}] \quad [1-13]$$

In the case of magnetics, $1/\mu$ is analogous to ρ and is called reluctivity. The reluctance, R_m , of a magnetic circuit, is shown in Equation [1-14].

$$R_m = \frac{MPL}{\mu_r \mu_o A_c} \quad [1-14]$$

Where MPL, is the magnetic path length, cm.

A_c is the cross-section of the core, cm^2 .

μ_r is the permeability of the magnetic material.

μ_o is the permeability of air.

A typical magnetic core is shown in Figure 1-27, illustrating the Magnetic Path Length (MPL) and the cross-sectional area, A_c , of a C core.

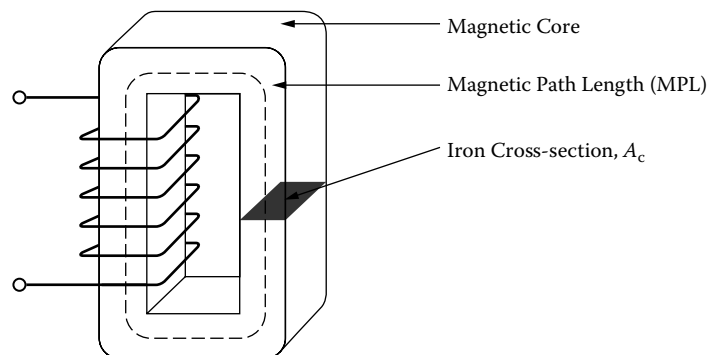


Figure 1-27. Magnetic Core Showing the Magnetic Path Length (MPL) and Iron Cross-section, A_c .

Air Gap

A high permeability material is one that has a low reluctance for a given magnetic path length (MPL) and iron cross-section, A_c . If an air gap is included in a magnetic circuit, as shown in Figure 1-28, which is otherwise composed of low reluctivity material like iron, almost all of the reluctance in the circuit will be at the gap. The reason for this is because the reluctivity of air is much greater than that of a magnetic material. For all practical purposes, controlling the size of the air gap controls the reluctance.

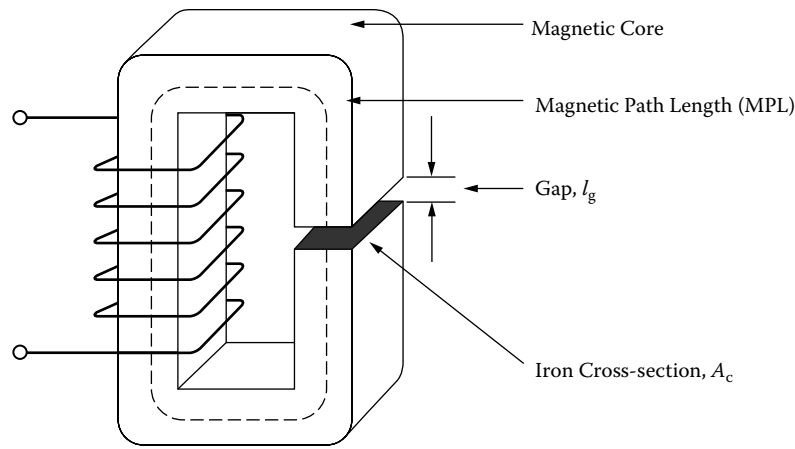


Figure 1-28. A Typical Magnetic Core with an Air Gap.

An example can best show this procedure. The total reluctance of the core is the sum of the iron reluctance and the air gap reluctance, in the same way that two series resistors are added in an electrical circuit. The equation for calculating the air gap reluctance, R_g , is basically the same as the equation for calculating the reluctance of the magnetic material, R_m . The difference is that the permeability of air is 1 and the gap length, l_g , is used in place of the Magnetic Path Length (MPL). The equation is shown in Equation [1-15].

$$R_g = \left(\frac{1}{\mu_o} \right) \left(\frac{l_g}{A_c} \right) \quad [1-15]$$

But, since $\mu_o = 1$, the Equation simplifies to:

$$R_g = \frac{l_g}{A_c} \quad [1-16]$$

Where:

l_g = the gap length, cm.

A_c = the cross-section of the core, cm^2 .

μ_o = the permeability of air.

The total reluctance, R_{mt} , for the core shown in Figure 1-28 is therefore:

$$R_{mt} = R_m + R_g$$

$$R_{mt} = \frac{MPL}{\mu_r \mu_o A_c} + \frac{l_g}{\mu_o A_c} \quad [1-17]$$

Where μ_r is the relative permeability, which is used exclusively with magnetic materials.

$$\mu_r = \frac{\mu}{\mu_o} = \frac{B}{\mu_o H}, \quad \left[\frac{\text{gauss}}{\text{oersteds}} \right] \quad [1-18]$$

The magnetic material permeability, μ_m , is given by:

$$\mu_m = \mu_r \mu_o \quad [1-19]$$

The reluctance of the gap is higher than that of the iron even when the gap is small. The reason is because the magnetic material has a relatively high permeability, as shown in Table 1-1. So the total reluctance of the circuit depends more on the gap than on the iron.

Table 1-1. Material Permeability

Material Permeability, μ_m	
Material Name	Permeability
Iron Alloys	0.8K to 25K
Ferrites	0.8K to 20K
Amorphous	0.8K to 80K

After the total reluctance, R_t , has been calculated, the effective permeability, μ_e , can be calculated.

$$R_{mt} = \frac{l_t}{\mu_e A_c}, \quad [1-20]$$

$$l_t = l_g + MPL$$

Where l_t is the total path length and μ_e is the effective permeability.

$$R_{mt} = \frac{l_t}{\mu_e A_c} = \frac{l_g}{\mu_o A_c} + \frac{MPL}{\mu_o \mu_r A_c} \quad [1-21]$$

Simplifying yields:

$$\frac{l_t}{\mu_e} = \frac{l_g}{\mu_o} + \frac{MPL}{\mu_o \mu_r} \quad [1-22]$$

Then:

$$\mu_e = \frac{l_t}{\frac{l_g}{\mu_o} + \frac{MPL}{\mu_o \mu_r}} \quad [1-23]$$

$$\mu_e = \frac{l_g + MPL}{\frac{l_g}{\mu_o} + \frac{MPL}{\mu_o \mu_r}}$$

If $l_g \ll \text{MPL}$, multiply both sides of the equation by $(\mu_r \mu_o \text{MPL})/(\mu_r \mu_o \text{MPL})$.

$$\mu_e = \frac{\mu_o \mu_r}{1 + \mu_r \left(\frac{l_g}{\text{MPL}} \right)} \quad [1-24]$$

The classic equation is:

$$\mu_e = \frac{\mu_m}{1 + \mu_m \left(\frac{l_g}{\text{MPL}} \right)} \quad [1-25]$$

Introducing an air gap, l_g , to the core cannot correct for the dc flux, but can sustain the dc flux. As the gap is increased, so is the reluctance. For a given magnetomotive force, the flux density is controlled by the gap.

Controlling the dc Flux with an Air Gap

There are two similar equations used to calculate the dc flux. The first equation is used with powder cores. Powder cores are manufactured from very fine particles of magnetic materials. This powder is coated with an inert insulation to minimize eddy currents losses and to introduce a distributed air gap into the core structure.

$$\begin{aligned} \mu_r &= \mu_e \\ B_{dc} &= (\mu_r) \left(\frac{0.4\pi NI}{\text{MPL}} \right), \quad [\text{gauss}] \\ \mu_r &= \frac{\mu_m}{1 + \mu_m \left(\frac{l_g}{\text{MPL}} \right)} \end{aligned} \quad [1-26]$$

The second equation is used, when the design calls for a gap to be placed in series with the Magnetic Path Length (MPL), such as a ferrite cut core, a C core, or butt-stacked laminations.

$$\begin{aligned} \mu_r &= \mu_e \\ B_{dc} &= (\mu_r) \left(\frac{0.4\pi NI}{\text{MPL}} \right), \quad [\text{gauss}] \end{aligned} \quad [1-27]$$

Substitute $(\text{MPL}\mu_m)/(\text{MPL}\mu_m)$ for 1:

$$\mu_r = \frac{\mu_m}{1 + \mu_m \left(\frac{l_g}{\text{MPL}} \right)} = \frac{\mu_m}{\frac{\text{MPL}\mu_m}{\text{MPL}\mu_m} + \mu_m \left(\frac{l_g}{\text{MPL}} \right)} \quad [1-28]$$

Then, simplify:

$$\mu_r = \frac{\text{MPL}}{\frac{\text{MPL}}{\mu_m} + l_g} \quad [1-29]$$

$$B_{dc} = \left(\frac{\text{MPL}}{\frac{\text{MPL}}{\mu_m} + l_g} \right) \left(\frac{0.4\pi NI}{\text{MPL}} \right), \quad [\text{gauss}] \quad [1-30]$$

Then, simplify:

$$B_{dc} = \frac{0.4\pi NI}{l_g + \frac{\text{MPL}}{\mu_m}}, \quad [\text{gauss}] \quad [1-31]$$

Types of Air Gaps

Basically, there are two types of gaps used in the design of magnetic components: bulk and distributed. Bulk gaps are maintained with materials, such as paper, Mylar, or even glass. The gapping materials are designed to be inserted in series with the magnetic path to increase the reluctance, R , as shown in Figure 1-29.

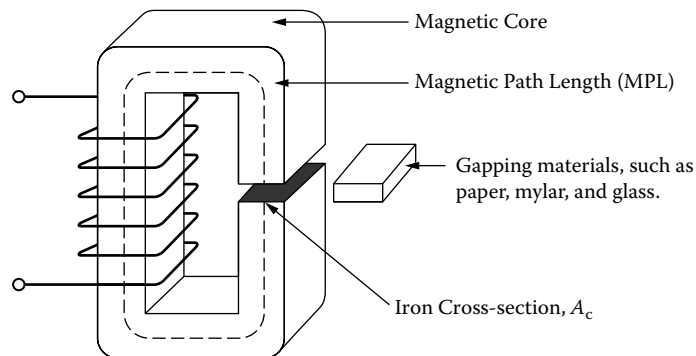


Figure 1-29. Placement of the Gapping Materials.

Placement of the gapping material is critical in keeping the core structurally balanced. If the gap is not proportioned in each leg, then the core will become unbalanced and create even more than the required gap. There are designs where it is important to place the gap in an area to minimize the noise that is caused by the fringing flux at the gap. The gap placement for different core configurations is shown in Figure 1-30. The standard gap placement is shown in Figure 1-30A, C, and D. The EE or EC cores shown in Figure 1-30B, are best-suited, when the gap has to be isolated within the magnetic assembly to minimize fringing flux noise. When the gap is used as shown in Figure 1-30A, C, and D, then, only half the thickness of the calculated gap dimension is used in each leg of the core.

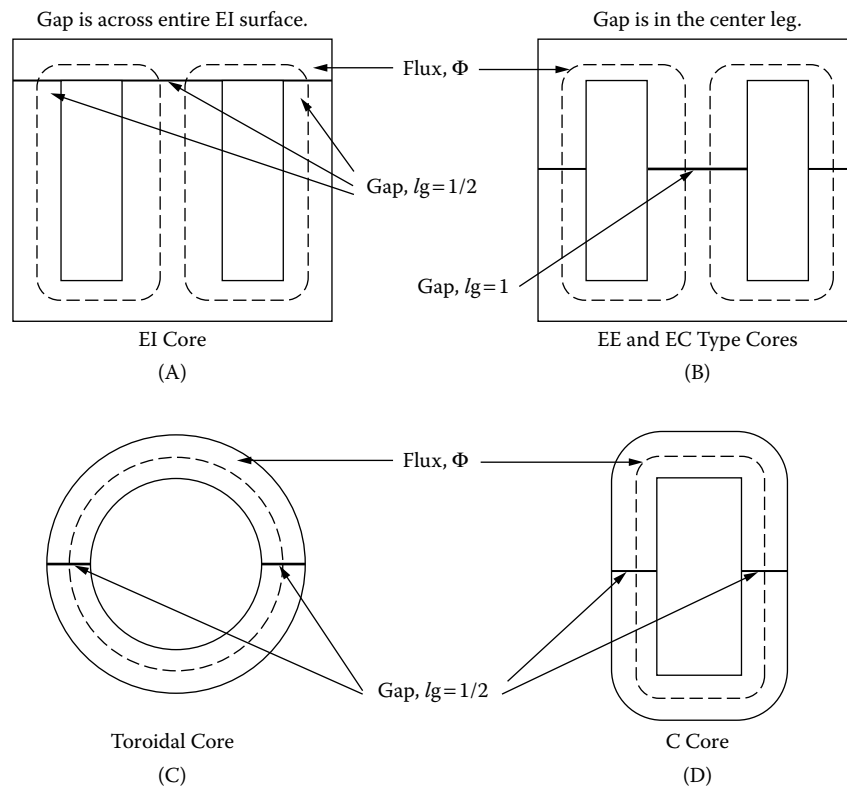


Figure 1-30. Gap Placement using Different Core Configurations.

Fringing Flux

Introduction

Fringing flux has been around since time began for the power conversion engineer. Designing power conversion magnetics that produce a minimum of fringing flux has always been a problem. Engineers have learned to design around fringing flux, and minimize its effects. It seems that when engineers do have a problem, it is usually at the time when the design is finished and ready to go. It is then that the engineer will observe something that was not recognized before. This happens during the final test when the unit becomes unstable, the inductor current is nonlinear, or the engineer just located a hot spot during testing. Fringing flux can cause a multitude of problems. Fringing flux can reduce the overall efficiency of the converter, by generating eddy currents that cause localized heating in the windings and/or the brackets. When designing inductors, fringing flux must be taken into consideration. If the fringing flux is not handled correctly, there will be premature core saturation. More and more magnetic components are now designed to operate in the sub-megahertz region. High frequency has really brought out the fringing flux and its parasitic eddy currents. Operating at high frequency has made the engineer very much aware of what fringing flux can do to hamper a design.

Material Permeability, (μ_m)

The B-H loops that are normally seen in the manufacturers' catalogs are usually taken from a toroidal sample of the magnetic material. The toroidal core, without a gap, is the ideal shape to view the B-H loop of a given material. The material permeability, μ_m , will be seen at its highest in the toroidal shape, as shown in Figure 1-31.

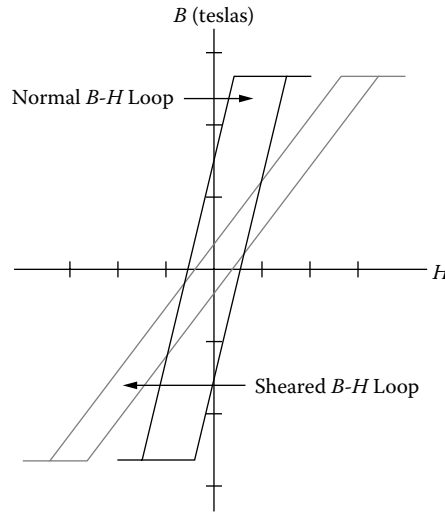


Figure 1-31. The Shearing of an Idealized B-H Loop due to an Air Gap.

A small amount of air gap, less than 25 microns, has a powerful effect by shearing over the B-H loop. This shearing over of the B-H loop reduces the permeability. High permeability ferrites that are cut, like E cores, have only about 80 percent of the permeability, than that of a toroid of the same material. This is because of the induced gap, even though the mating surfaces are highly polished. In general, magnetic materials with high-permeability, are sensitive to temperature, pressure, exciting voltage, and frequency. The inductance change is directly proportional to the permeability change. This change in inductance will have an effect on the exciting current. It is very easy to see, that inductors that are designed into an LC, tuned circuit, must have a stable permeability, μ_c .

$$L = \frac{0.4\pi N^2 A_c \Delta\mu (10^{-8})}{MPL}, \text{ [henrys]} \tag{1-32}$$

Air Gaps

Air gaps are introduced into magnetic cores for a variety of reasons. In a transformer design a small air gap, l_g , inserted into the magnetic path, will lower and stabilize the effective permeability, μ_c .

$$\mu_e = \frac{\mu_m}{1 + \mu_m \left(\frac{l_g}{MPL} \right)} \quad [1-33]$$

This will result in a tighter control of the permeability change with temperature, and exciting voltage. Inductor designs will normally require a large air gap, l_g , to handle the dc flux.

$$l_g = \frac{0.4\pi N I_{dc} (10^{-4})}{B_{dc}}, \quad [\text{cm}] \quad [1-34]$$

Whenever an air gap is inserted into the magnetic path, as shown in Figure 1-32, there is an induced, fringing flux at the gap.

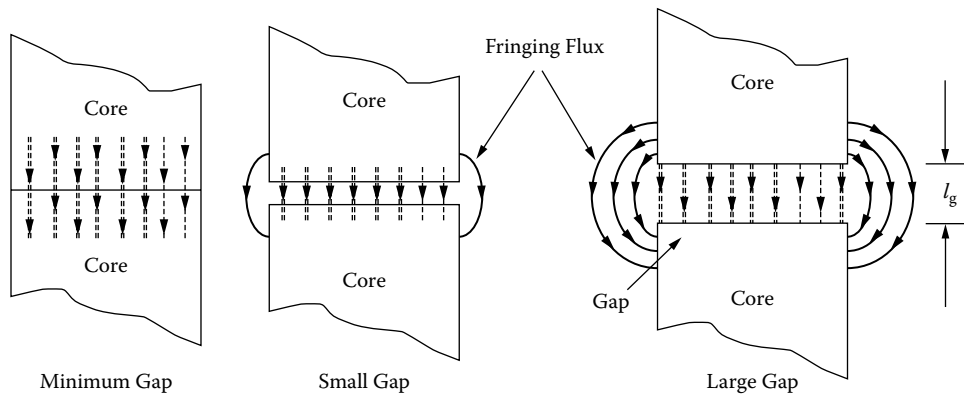


Figure 1-32. Fringing Flux at the Gap.

The fringing flux effect is a function of gap dimension, the shape of the pole faces, and the shape, size, and location of the winding. Its net effect is to shorten the air gap. Fringing flux decreases the total reluctance of the magnetic path and, therefore, increases the inductance by a factor, F , to a value greater than the one calculated.

Fringing Flux, F

Fringing flux is completely around the gap and re-enters the core in a direction of high loss, as shown in Figure 1-33. Accurate prediction of gap loss, P_g , created by fringing flux is very difficult to calculate.

This area around the gap is very sensitive to metal objects, such as clamps, brackets and banding materials. The sensitivity is dependent on the intensity of the magnetomotive force, gap dimensions and the operating frequency. If a metal bracket or banding material is used to secure the core, and it passes over the gap, two things can happen: (1) If the material ferromagnetic is placed over the gap, or is in close proximity so it conducts the magnetic field, this is called “shorting the gap.” Shorting the gap is the same as reducing the gap

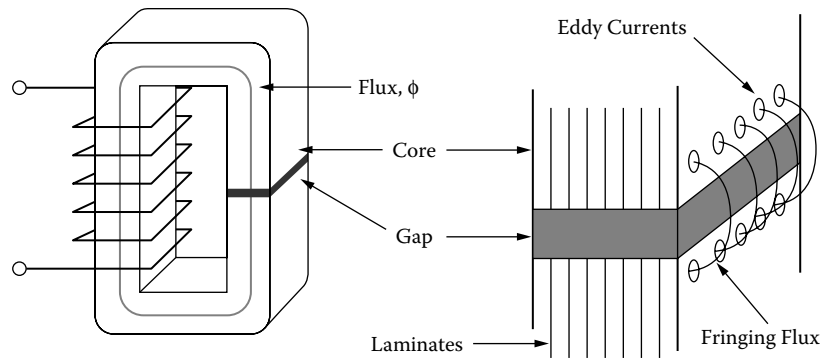


Figure 1-33. Fringing Flux, with High Loss Eddy Currents.

dimension, thereby producing a higher inductance, than designed, and could drive the core into saturation. (2) If the material is metallic, (such as copper, or phosphor bronze), but not ferromagnetic, it will not short the gap or change the inductance. In both cases, if the fringing flux is strong enough, it will induce eddy currents that will cause localized heating. This is the same principle used in induction heating.

Gapped, dc Inductor Design

The fringing flux factor, F, has an impact on the basic inductor design equations. When the engineer starts a design, he or she must determine the maximum values for B_{dc} and for B_{ac} , which will not produce magnetic saturation. The magnetic material that has been selected will dictate the saturation flux density. The basic equation for maximum flux density is:

$$B_{max} = \frac{0.4\pi N \left(I_{dc} + \frac{\Delta I}{2} \right) (10^{-4})}{l_g + \frac{MPL}{\mu_m}}, \quad [\text{teslas}] \quad [1-35]$$

The inductance of an iron-core inductor, carrying dc and having an air gap, may be expressed as:

$$L = \frac{0.4\pi N^2 A_c (10^{-8})}{l_g + \frac{MPL}{\mu_m}}, \quad [\text{henrys}] \quad [1-36]$$

The inductance is dependent on the effective length of the magnetic path, which is the sum of the air gap length, l_g , and the ratio of the core magnetic path length to the material permeability, (MPL/μ_m) . The final determination of the air gap size requires consideration of the fringing flux effect which is a function of the gap dimension, the shape of the pole faces, and the shape, size, and location of the winding. The winding length, or the G dimension of the core, has a big influence on the fringing flux. See, Figure 1-34 and Equation 1-37.

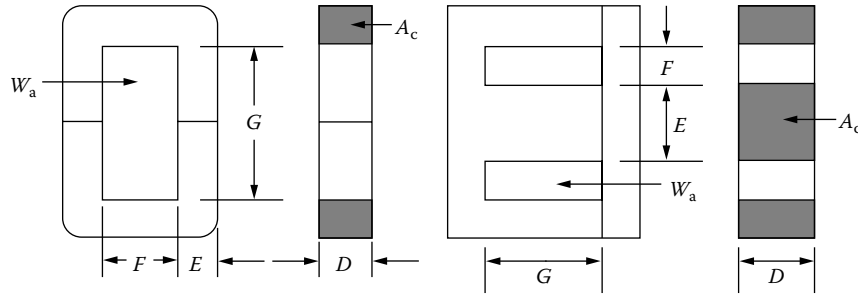


Figure 1-34. Dimensional, Call Out for C and E Cores.

The fringing flux decreases the total reluctance of the Magnetic Path Length and, therefore, increases the inductance by a factor of F to a value greater than that calculated. The fringing flux factor is:

$$F = \left(1 + \frac{l_g}{\sqrt{A_c}} \ln \frac{2G}{l_g} \right) \quad [1-37]$$

After the inductance has been calculated using Equation 1-36, the fringing flux factor has to be incorporated into Equation 1-36. Equation 1-36 can now be rewritten to include the fringing flux factor, as shown in Equation 1-38

$$L = F \left(\frac{0.4\pi N^2 A_c (10^{-8})}{l_g + \frac{MPL}{\mu_m}} \right), \quad [\text{henrys}] \quad [1-38]$$

The fringing flux factor, F, can now be included into Equation 1-35. This will check for premature, core saturation.

$$B_{\max} = F \left(\frac{0.4\pi N \left(I_{dc} + \frac{\Delta I}{2} \right) (10^{-4})}{l_g + \frac{MPL}{\mu_m}} \right), \quad [\text{teslas}] \quad [1-39]$$

Now that the fringing flux factor, F, is known and inserted into Equation 1-38. Equation 1-38 can be rewritten to solve for the required turns so that premature core saturation will not happen, as shown in Equation 1-40.

$$N = \sqrt{\frac{L \left(l_g + \frac{MPL}{\mu_m} \right)}{0.4\pi A_c F (10^{-8})}}, \quad [\text{turns}] \quad [1-40]$$

Fringing Flux and Coil Proximity

As the air gap increases, the fringing flux will increase. Fringing flux will fringe out away from the gap by the distance of the gap. If a coil was wound tightly around the core and encompasses the gap, the flux generated

around the magnet wire will force the fringing flux back into the core. The end result will not produce any fringing flux at all, as shown in Figure 1-35. As the coil distance moves away from the core, the fringing flux will increase until the coil distance from the core is equal to the gap dimension.

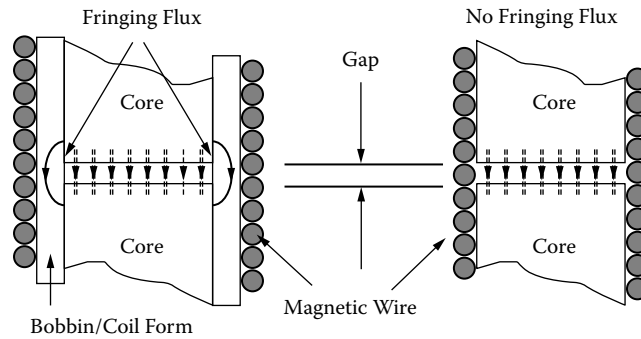


Figure 1-35. Comparing a Tightly-Wound Coil, and a Coil Wound on a Coil Form.

Fringing Flux, Crowding

Flux will always take the path of highest permeability. This can best be seen in transformers with interleaved laminations. The flux will traverse along the lamination until it meets its mating, I or E. At this point, the flux will jump to the adjacent lamination and bypass the mating point, as shown in Figure 1-36.

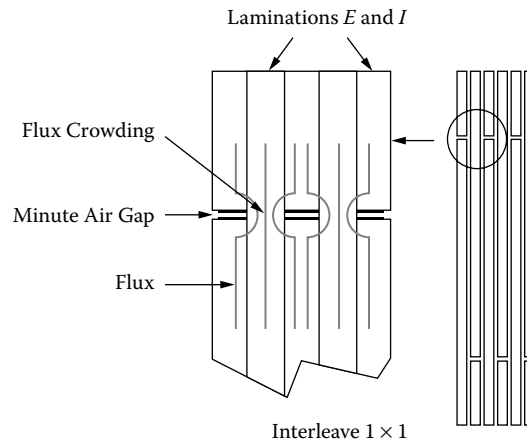


Figure 1-36. Flux Crowding in Adjacent Laminations.

This phenomena can best be seen by observing the exciting current at low, medium and high flux levels, as shown in Figure 1-37. At low levels of excitation, the exciting current is almost square, due to the flux taking the high permeability path, by jumping to the adjacent lamination, as shown in Figure 1-36. As the excitation is increased, the adjoining lamination will start to saturate, and the exciting current will increase and become nonlinear. When the adjacent lamination approaches saturation, the permeability drops. It is then that the flux will go in a straight line and cross the minute air gap, as shown in Figure 1-36.

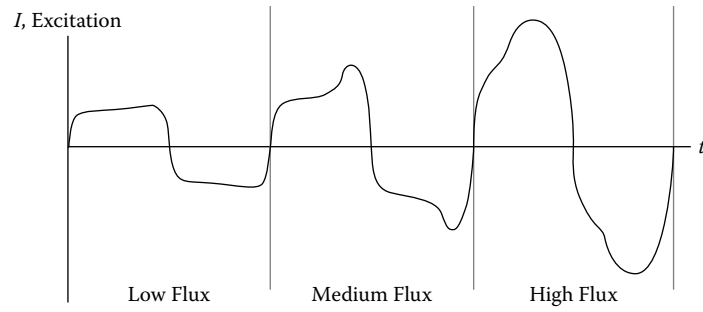


Figure 1-37. Exciting Current, at Different Levels of Flux Density, B.

Fringing Flux and Powder Cores

Designing high frequency converters, using low permeability powder cores, will usually require very few turns. Low perm powder cores (less than 60), exhibit fringing flux. Powder cores with a distributed gap will have fringing flux that shorts the gap and gives the impression of a core with a higher permeability. Because of the fringing flux and a few turns, it is very important to wind uniformly and in a consistent manner. This winding is done to control the fringing flux and get inductance repeatability from one core to another, as shown in Figures 1-38 and 1-39.

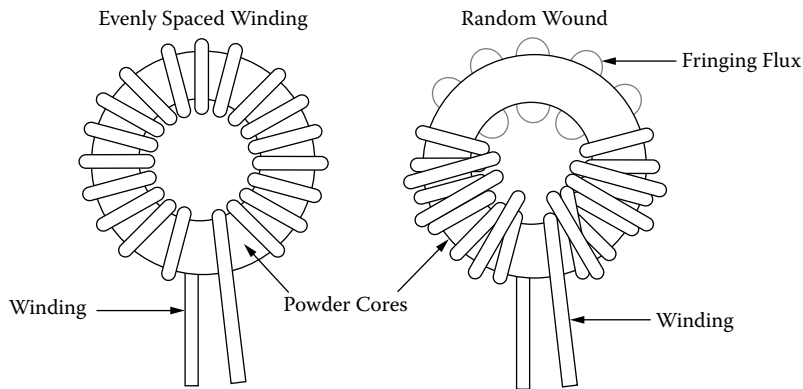


Figure 1-38. Comparing Toroidal, Winding Methods.

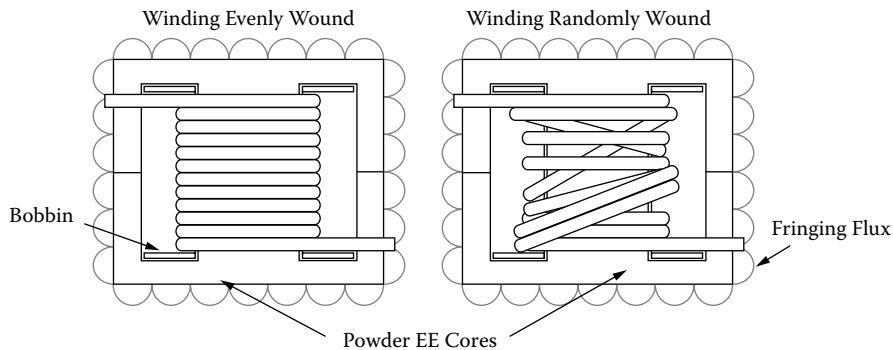


Figure 1-39. Comparing EE Cores, Winding Methods.

Chapter 2

Magnetic Materials and Their Characteristics

Table of Contents

1. Introduction.....	2-3
2. Saturation	2-3
3. Remanence Flux, B_r , and Coercivity H_c	2-4
4. Permeability, μ	2-4
5. Hysteresis Loss, Resistivity, ρ , (core loss)	2-4
6. Introduction to Silicon Steel	2-5
7. Introduction to Thin Tape Nickel Alloys.....	2-5
8. Introduction to Metallic Glass.....	2-9
9. Introduction to Soft Ferrites.....	2-12
10. Manganese-Zinc Ferrites	2-13
11. Nickel-Zinc Ferrites	2-13
12. Ferrite Cross Reference.....	2-16
13. Introduction to Molypermalloy Powder Cores	2-17
14. Introduction to Iron Powder Cores.....	2-17
15. Core Loss	2-24
16. Core Loss Equations.....	2-25
17. Selection of Magnetic Materials	2-29
18. Typical Operation	2-29
19. Material Characteristics	2-30
20. Magnetic Material Saturation Defined	2-33
21. Test Conditions	2-36
22. Magnetic Material Saturation Theory.....	2-41
23. Air Gap Effect.....	2-42
24. Effect of Gapping.....	2-42
25. Composite Core Configuration	2-50
26. Summary	2-53

Introduction

The magnetic material is the paramount player in the design of magnetic components. The magnetics design engineer has three standard words when making the normal design trade-off study: cost, size, and performance. He will be happy to stuff any two into the bag. The magnetics engineer is now designing magnetic components that operate from below the audio range to the megahertz range. He is normally asked to design for maximum performance, with the minimum of his parasitic friends' capacitance and leakage inductance. Today, the magnetic materials the engineer has to work with are silicon steel, nickel iron (permalloy), cobalt iron (permendur), amorphous metallic alloys, and ferrites. These also have spin-off material variants, such as moly-permalloy powder, sendust powder, and iron powder cores. From this group of magnetic materials, the engineer will make trade-offs with the magnetic properties for his design. These properties are: saturation, B_s , permeability, μ , resistivity, ρ (core loss), remanence, B_r , and coercivity, H_c .

Saturation

A typical hysteresis loop of a soft magnetic material is shown in Figure 2-1. When a high magnetizing force is encountered, a point is reached where further increase in, H , does not cause useful increase in, B . This point is known as the saturation point of that material. The saturation flux density, B_s , and the required magnetizing force, H_s , to saturate the core are shown with dashed lines.

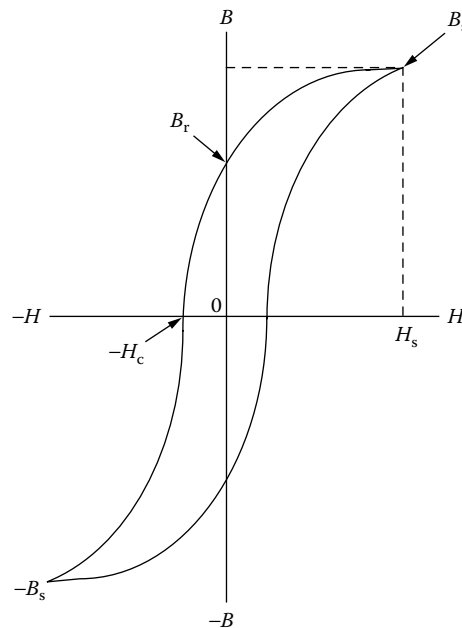


Figure 2-1. Typical B-H or Hysteresis Loop of a Soft Magnetic Material.

Remanence Flux, B_r , and Coercivity H_c

In Figure 2-1 the hysteresis loop clearly shows the remanence flux density, B_r . The remanence flux is the polarized flux remaining in the core after the excitation has been removed. The magnetizing force, $-H_c$, is called coercivity. It is the amount of magnetizing force required to bring the remanence flux density back to zero.

Permeability, μ

The permeability of a magnetic material is a measure of the ease in magnetizing the material. Permeability, μ , is the ratio of the flux density, B , to the magnetizing force, H , as shown in Equation [2-1].

$$\mu = \frac{B}{H}, \quad [\text{permeability}] \quad [2-1]$$

The relationship between B and H is not linear, as shown in the hysteresis loop in Figure 2-1. Then, it is evident that the ratio, B/H , (permeability), also varies. The variation of permeability with flux density, B , is shown in Figure 2-2. Also, it shows the flux density at which the permeability is at a maximum.

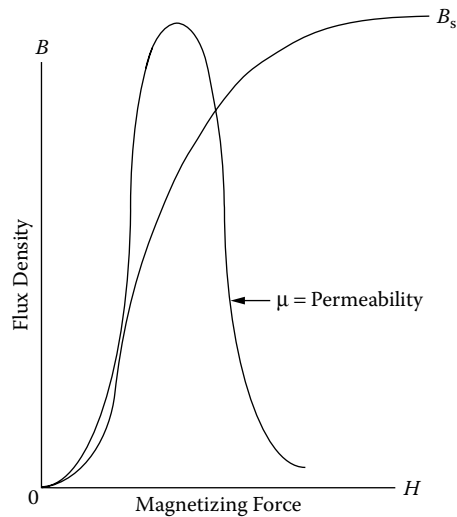


Figure 2-2. Variation in Permeability μ with B and H .

Hysteresis Loss, Resistivity, ρ , (core loss)

The enclosed area within the hysteresis, shown in Figure 2-1, is a measure of the energy lost in the core material during that cycle. This loss is made up in two components: (1) the hysteresis loss and (2) eddy current loss. The hysteresis loss is the energy loss when the magnetic material is going through a cycling state. The

eddy current loss is caused when the lines of flux pass through the core, inducing electrical currents in it. These currents are called eddy currents and produce heat in the core. If the electrical resistance of the core is high, the current will be low; therefore, a feature of low-loss material is high electrical resistance. In the norm, when designing magnetic components, the core loss is a major design factor. Core loss can be controlled by selecting the right material and thickness. Selecting the correct material, and operating within its limits, will prevent overheating that could result in damage to the wire insulation and/or the potting compound.

Introduction to Silicon Steel

Silicon steel was one of the first alloys to be used in transformers and inductors. It has been greatly improved over the years and is probably, pound for pound, the most widely used magnetic material. One of the drawbacks in using steel in the early years was, as the material became older, the losses would increase. With the addition of silicon to the steel, the advantages were twofold: it increased the electrical resistivity, therefore reducing the eddy current losses, and it also improved the material's stability with age.

Silicon steel offers high saturation flux density, a relatively good permeability at high flux density, and a moderate loss at audio frequency. One of the important improvements made to the silicon steel was in the process called cold-rolled, grain-oriented, AISI type M6. This M6 grain-oriented steel has exceptionally low losses and high permeability. It is used in applications requiring high performance and the losses will be at a minimum.

Introduction to Thin Tape Nickel Alloys

High permeability metal alloys are based primarily on the nickel-iron system. Although Hopkinson investigated nickel-iron alloys as early as 1889, it was not until the studies by Elmen, starting in about 1913, on properties in weak magnetic fields and effects of heat-treatments, that the importance of the Ni-Fe alloys was realized. Elmen called his Ni-Fe alloys, "Permalloys," and his first patent was filed in 1916. His preferred composition was the 78Ni-Fe alloy. Shortly after Elmen, Yensen started an independent investigation that resulted in the 50Ni-50Fe alloy, "Hipernik," which has lower permeability and resistivity but higher saturation than the 78-Permalloy, (1.5 teslas compared to 0.75 teslas), making it more useful in power equipment.

Improvements in the Ni-Fe alloys were achieved by high temperature anneals in hydrogen atmosphere, as first reported by Yensen. The next improvement was done by using grain-oriented material and annealing it, in a magnetic field, which was also in a hydrogen atmosphere. Kelsall and Bozorth did this work. Using these two methods, a new material, called Supermalloy, was achieved. It has a higher permeability, a lower coercive force, and about the same flux density as 78-Permalloy. Perhaps the most important of these factors is the

magnetic anneal, which, not only increases permeability, but also provides a “square” magnetization curve, important in high frequency power conversion equipment.

In order to obtain high resistance, and therefore lower core losses for high frequency applications, two approaches have been followed: (1) modification of the shape of metallic alloys and (2) development of magnetic oxides. The result was the development of thin tapes and powdered alloys in the 1920's, and thin films in the 1950's. The development of thin film has been spurred by the requirements of aerospace, power conversion electronics from the mid 1960's to the present.

The Ni-Fe alloys are available in thicknesses of 2 mil, 1 mil, 0.5 mil, 0.25 and 0.125 mil. The material comes with a round or square B-H loop. This gives the engineer a wide range of sizes and configurations from which to select for a design. The iron alloy properties for some of the most popular materials are shown in Table 2-1. Also, given in Table 2-1, is the Figure number for the B-H loop of each of the magnetic materials.

Table 2-1. Magnetic Properties for Selected Iron Alloys Materials

Iron Alloy Material Properties								
Material Name	Composition	Initial Permeability μ_i	Flux Density Teslas B_s	Curie Temp. °C	dc, Coercive Force, Hc Oersteds	Density grams/cm ³ δ	Weight Factor x	Typical B-H Loop Figures
Silicon	3% Si 97% Fe	1.5 K	1.5-1.8	750	0.4-0.6	7.63	1.000	(2-3)
Supermendur*	49% Co 49% Fe 2% V	0.8 K	1.9-2.2	940	0.15-0.35	8.15	1.068	(2-4)
Orthonol	50% Ni 50% Fe	2 K	1.42-1.58	500	0.1-0.2	8.24	1.080	(2-5)
Permalloy	79% Ni 17% Fe 4% Mo	12 K-100 K	0.66-0.82	460	0.02-0.04	8.73	1.144	(2-6)
Supermalloy	78% Ni 17% Fe 5% Mo	10 K-50 K	0.65-0.82	460	0.003-0.008	8.76	1.148	(2-7)
* Field Anneal. x Silicon has unity weight factor.								

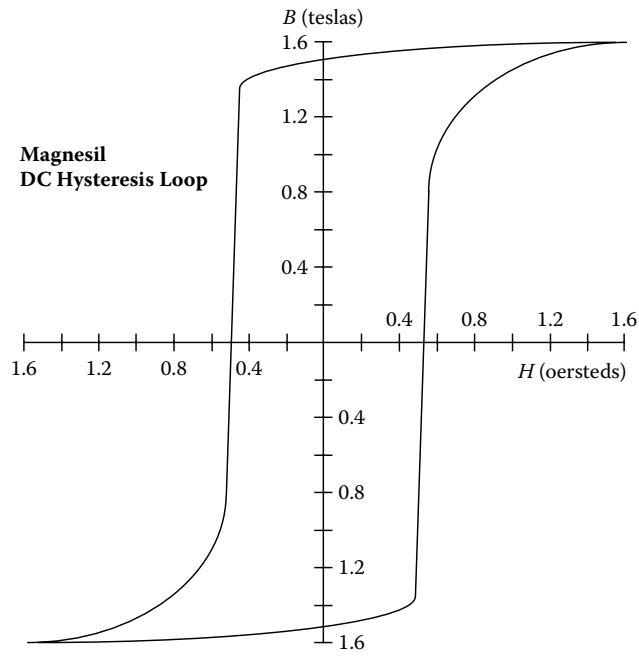


Figure 2-3. Silicon B-H Loop: 97% Fe 3% Si.

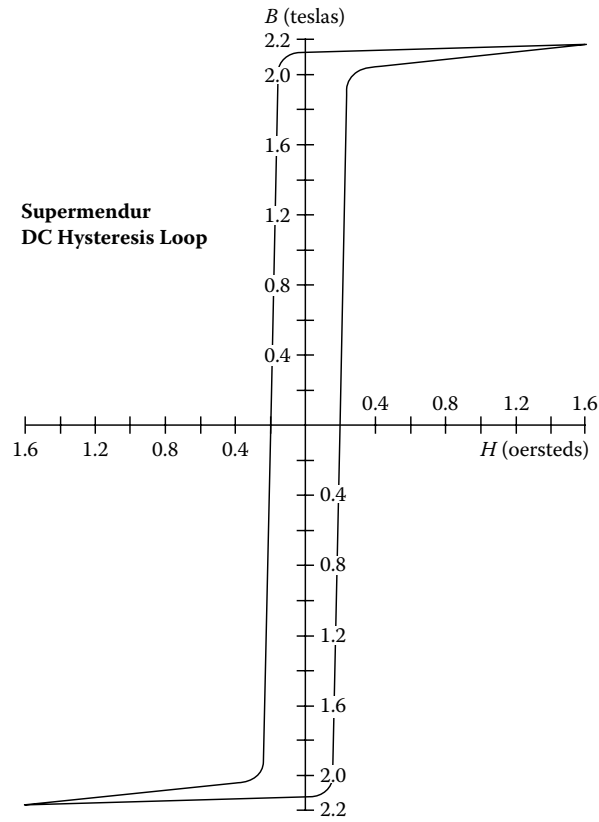


Figure 2-4. Supermendur B-H Loop: 49% Fe 49% Co 2% V.

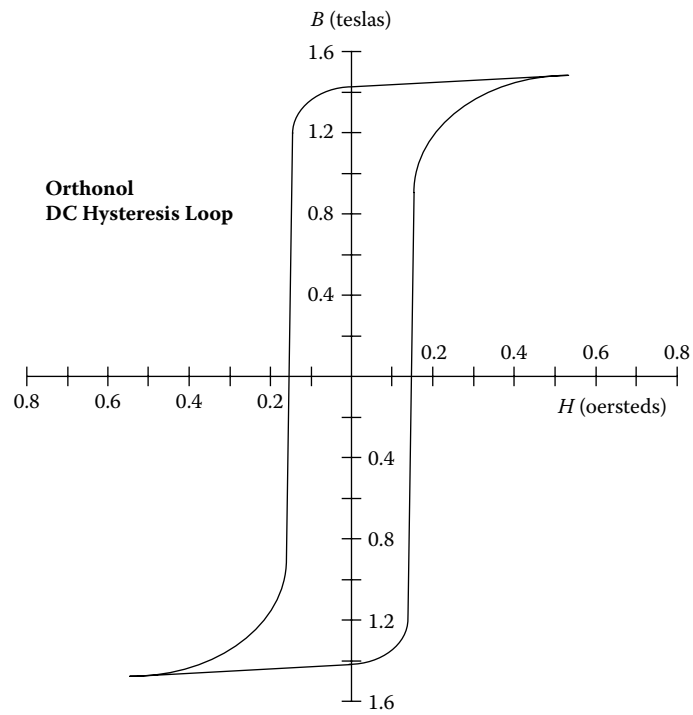


Figure 2-5. Orthonol B-H Loop: 50% Fe 50% Ni.

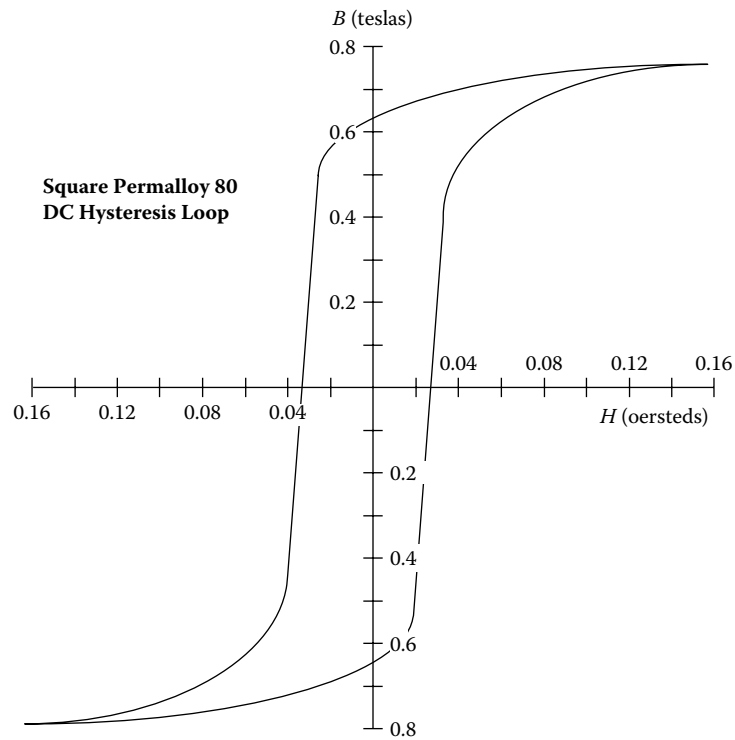


Figure 2-6. Square Permalloy 80 B-H Loop: 79% Ni 17% Fe 4% Mo.

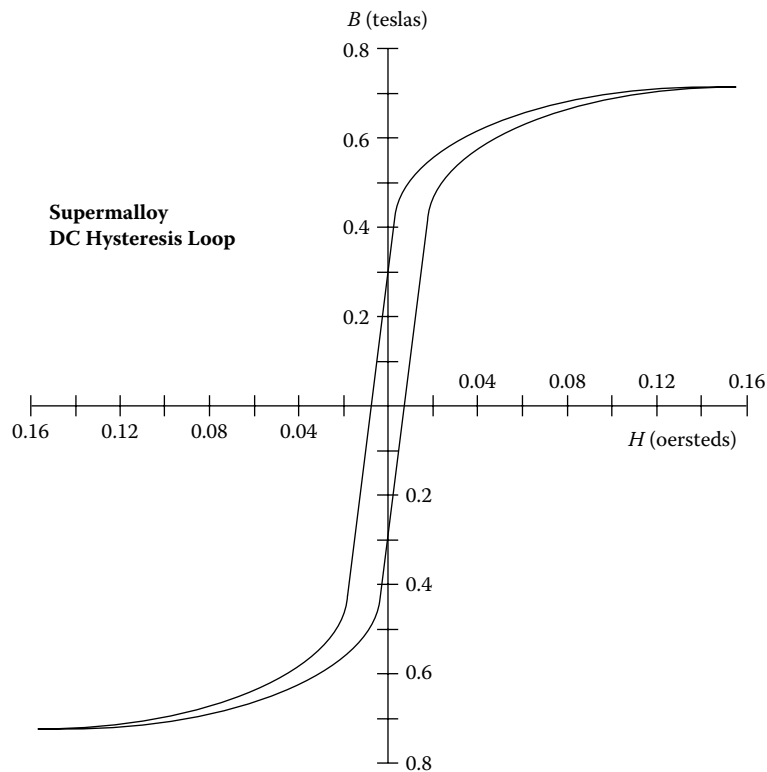


Figure 2-7. Supermalloy B-H Loop: 78% Ni 17% Fe 5% Mo.

Introduction to Metallic Glass

The first synthesis of a metallic glass drawing wide attention among material scientists, occurred in 1960. Klement, Willens and Duwez reported that a liquid, AuSi alloy, when rapidly quenched to liquid nitrogen temperature, would form an amorphous solid. It was twelve years later that Chen and Polk produced ferrous-based metallic glasses in useful shapes with significant ductility. Metallic glasses have since survived the transition from laboratory curiosities to useful products, and currently are the focus of intensive technological and fundamental studies.

Metallic glasses are generally produced, by liquid quenching, in which a molten metal alloy is rapidly cooled, at rates on the order of 10^5 degrees/sec., through the temperature at which crystallization normally occurs. The basic difference between crystalline (standard magnetic material) and glassy metals is in their atomic structures. Crystalline metals are composed of regular, three-dimensional arrays of atoms, which exhibit long-range order. Metallic glasses do not have long-range structural order. Despite their structural differences, crystalline and glassy metals of the same compositions exhibit nearly the same densities.

The electrical resistivities of metallic glasses are much larger, (up to three times higher), than those of crystalline metals of similar compositions. The magnitude of the electrical resistivities and their temperature coefficients in the glassy and liquid states are almost identical.

Metallic glasses are quite soft magnetically. The term, “soft,” refers to a large response of the magnetization to a small-applied field. A large magnetic response is desirable in such applications as transformers and inductors. The obvious advantages of these new materials are in high frequency applications with their high induction, high permeability, and low core loss.

There are four amorphous materials that have been used in high frequency applications: 2605SC, 2714A, 2714AF and Vitroperm 500F. Material 2605SC offers a unique combination of high resistivity, high saturation induction, and low core loss, making it suitable for designing high frequency dc inductors. Material 2714A is a cobalt material that offers a unique combination of high resistivity, high squareness ratio B_r/B_s , and very low core loss, making it suitable for designing high frequency aerospace transformers and mag-amps. The Vitroperm 500F is an iron based material with a saturation of 1.2 teslas and is well-suited for high frequency transformers and gapped inductors. The high frequency core loss for the nanocrystalline 500F is lower than some ferrite, even operating at a high flux density. The amorphous properties for some of the most popular materials are shown in Table 2-2. Also, given in Table 2-2, is the Figure number for the B-H loop of each of the magnetic materials.

Table 2-2. Magnetic Properties for Selected Amorphous Materials

Amorphous Material Properties								
Material Name	Major Composition	Initial Permeability μ_i	Flux Density Telsas B_s	Curie Temperature °C	dc, Coercive Force, Hc Oersteds	Density grams/cm ³ δ	Weight Factor x	Typical B-H Loop Figures
2605SC	81% Fe 13.5% B 3.5% Si	1.5K	1.5-1.6	370	0.4-0.6	7.32	0.957	(2-8)
2714A	66% Co 15% Si 4% Fe	0.8K	0.5-0.65	205	0.15-0.35	7.59	0.995	(2-9)
2714AF	66% Co 15% Si 4% Fe	2K	0.5-0.65	205	0.1-0.2	7.59	0.995	(2-10)
Nanocrystal Vitroperm 500F*	73.5% Fe 1% Cu 15.5% Si	30K-80K	1.0-1.2	460	0.02-0.04	7.73	1.013	(2.11)

* Vitroperm is the trademark of Vacuumschmelze.
x Silicon has a unity weight factor. See Table 2.1.

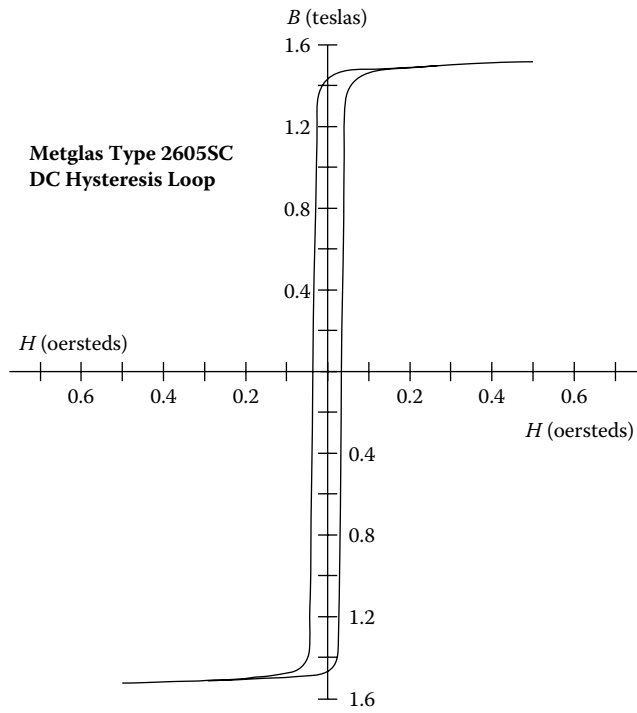


Figure 2-8. Amorphous 2605SC B-H Loop: 81% Fe 13.5% B 3.5% Si.

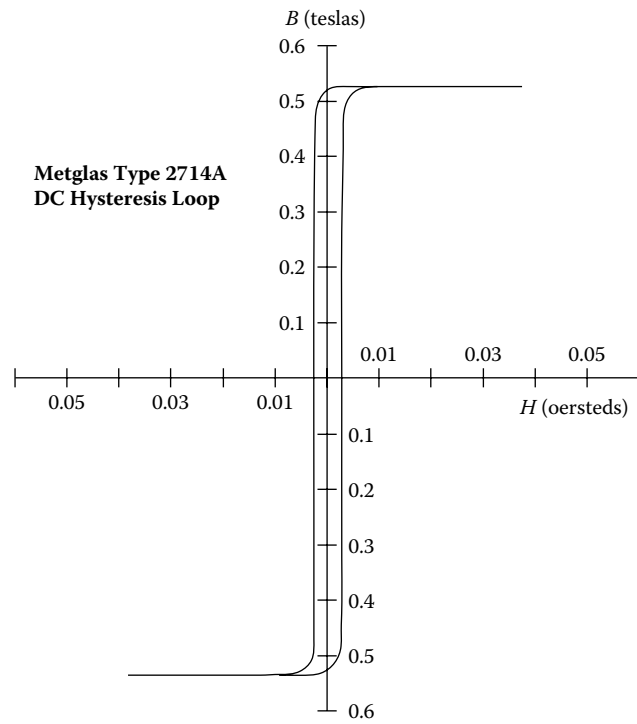


Figure 2-9. Amorphous 2714A B-H Loop: 66% Co 15% Si 4% Fe.

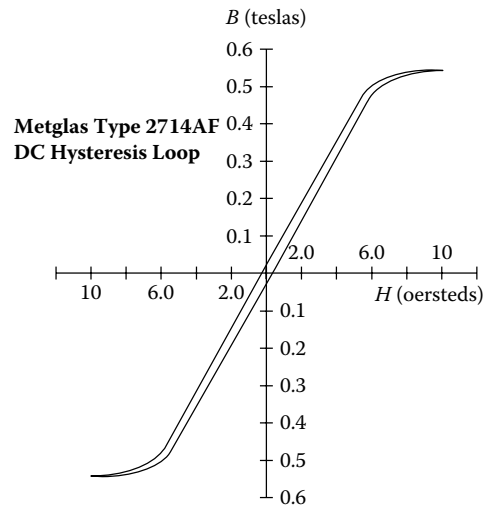


Figure 2-10. Amorphous 2714AF B-H Loop: 66% Co 15% Si 4% Fe.

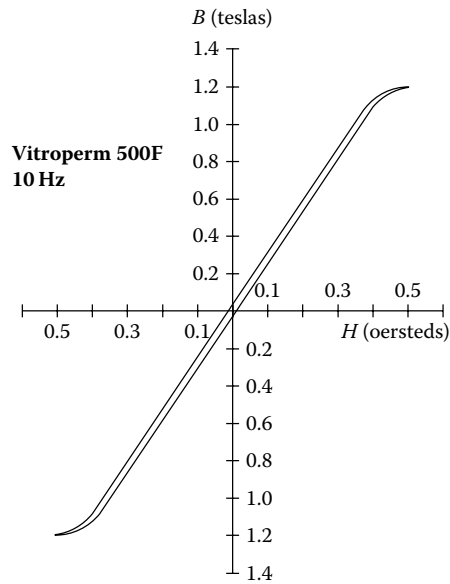


Figure 2-11. Vitroperm 500F B-H Loop: 73.5% Fe 15.5% Si 1% Cu.

Introduction to Soft Ferrites

In the early days of electrical industry, the need for the indispensable magnetic material was served by iron and its magnetic alloys. However, with the advent of higher frequencies, the standard techniques of reducing eddy current losses, (using laminations or iron powder cores), was no longer efficient or cost effective.

This realization stimulated a renewed interest in “magnetic insulators,” as first reported by S. Hilpert in Germany, in 1909. It was readily understood that, if the high electrical resistivity of oxides could be combined with desired magnetic characteristics, a magnetic material that was particularly well-suited for high frequency operation would result.

Research to develop such a material was being performed by scientists in various laboratories all over the world, such as V. Kato, T. Takei, and N. Kawai in the 1930's in Japan, and by J. Snoek of the Philips' Research Laboratories in the period 1935-1945 in The Netherlands. By 1945, Snoek had laid down the basic fundamentals of the physics and technology of practical ferrite materials. In 1948, the Neel Theory of ferromagnetism provided the theoretical understanding of this type of magnetic material.

Ferrites are ceramic, homogeneous materials composed of oxides; iron oxide is their main constituent. Soft ferrites can be divided into two major categories; manganese-zinc and nickel-zinc. In each of these categories, changing the chemical composition, or manufacturing technology, can manufacture many different Mn-Zn and Ni-Zn material grades. The two families of Mn-Zn and Ni-Zn ferrite materials complement each other, and allow the use of soft ferrites from audio frequencies to several hundred megahertz. Manufacturers do not like to handle manganese-zinc in the same area, or building with nickel-zinc, because one contaminates the other, which leads to poor performance yields. The basic difference between manganese-zinc and nickel-zinc is shown in Table 2-3. The biggest difference is manganese-zinc has a higher permeability and nickel-zinc has a higher resistivity. Shown in Table 2-4 are some of the most popular and new ferrite materials. Also, given in Table 2-4, is the Figure number for the B-H loop of each of the materials.

Table 2-3. Comparing Manganese-Zinc and Nickel-Zinc Basic Properties

Basic Ferrite Material Properties					
Materials	Initial Permeability μ_i	Flux Density B_{max} Teslas	Curie Temperature, °C	dc, Coercive Force, H_c Oersteds	Resistivity Ω - cm
Manganese Zinc	750-15 K	0.3-0.5	100-300	0.04-0.25	10-100
Nickel Zinc	15-1500	0.3-0.5	150-450	0.3-0.5	10^6

Manganese-Zinc Ferrites

This type of soft ferrite is the most common, and is used in many more applications than the nickel-zinc ferrites. Within the Mn-Zn category, a large variety of materials are possible. Manganese-zinc ferrites are primarily used at frequencies less than 2 MHz.

Nickel-Zinc Ferrites

This class of soft ferrite is characterized by its high material resistivity, several orders of magnitude higher than Mn-Zn ferrites. Because of its high resistivity, Ni-Zn ferrite is the material of choice for operating from 1-2 MHz to several hundred megahertz.

The material permeability, μ_m , has little influence on the effective permeability, μ_e , when the gap dimension is relatively large, as shown in Table 2-5.

Table 2-4. Magnetic Properties for Selected Ferrite Materials

Ferrites Material Properties							
*Magnetics Material Name	Initial Permeability μ_i	Flux Density Teslas $B_s@15 \text{ Oe}$	Residual Flux Teslas B_r	Curie Temperature $^{\circ}\text{C}$	dc, Coercive Force, H_c Oersteds	Density grams/cm ³ δ	Typical B-H Loop Figures
L	900	0.42 T	0.15 T	>300	0.94	4.8	(2-12)
R	2300	0.50 T	0.12 T	>230	0.18	4.8	(2-13)
P	2500	0.50 T	0.12 T	>230	0.18	4.8	(2-13)
T	2300	0.47 T	0.16 T	>215	0.25	4.8	NA
F	5000	0.49 T	0.10 T	>250	0.2	4.8	(2-14)
W	10,000	0.43 T	0.07 T	>125	0.15	4.8	(2-15)

* Magnetics, a Division of Spang & Company.

Table 2-5. Permeability, and Its Effect on Gapped Inductors

Comparing Material Permeabilities					
*Material	μ_m	Gap, inch	Gap, cm	**MPL, cm	μ_e
L	900	0.04	0.101	10.4	92
R	2300	0.04	0.101	10.4	98
P	2500	0.04	0.101	10.4	99
F	3000	0.04	0.101	10.4	100

* The materials are from Magnetics, a Division of Spang & Company.
 ** Core, ETD44.

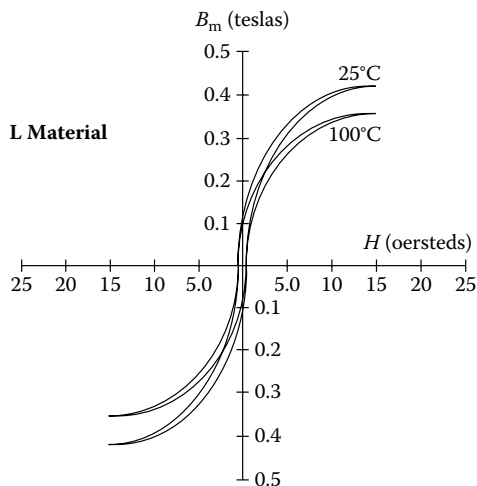


Figure 2-12. Ferrite B-H Loop, L Material at 25 and 100°C.

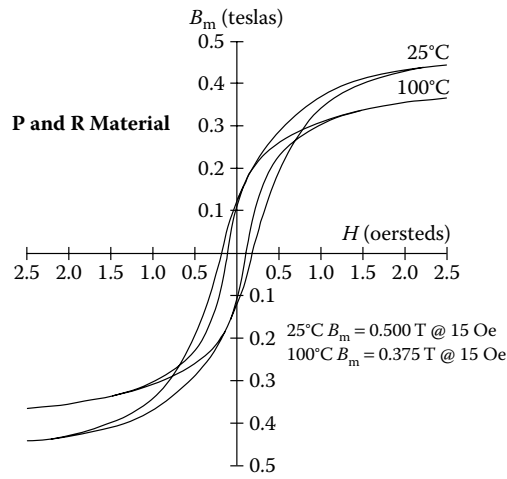


Figure 2-13. Ferrite B-H Loop, P & R Material at 25 and 100°C.

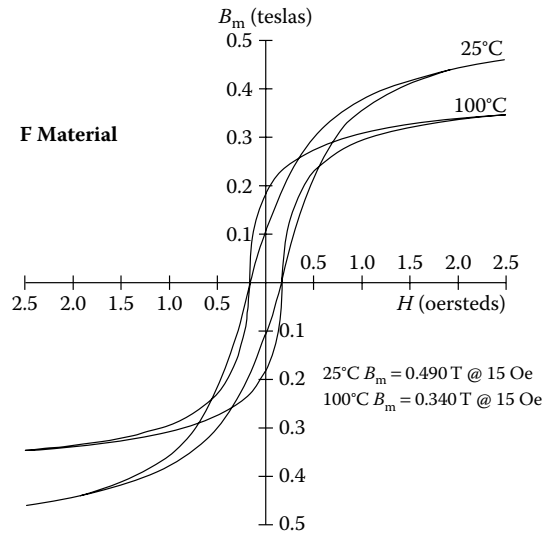


Figure 2-14. Ferrite B-H Loop, F Material at 25 and 100°C.

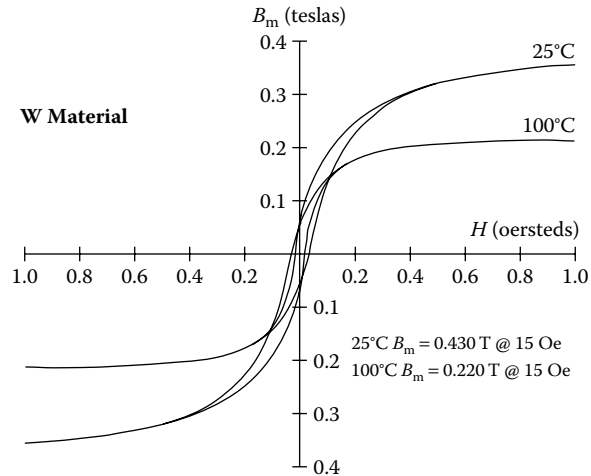


Figure 2-15. Ferrite B-H Loop, W & H Material at 25 and 100°C.

Ferrite Cross Reference

A similar ferrite cross-reference has been made in Table 2-6. This table has been put together using some of the leading ferrite manufacturers. The ferrite materials in Table 2-6 have been organized for materials best suited for power transformers, power inductors and common-mode filters.

Table 2-6. Similar Ferrite Materials Best Suited for Power and Filters

Similar Ferrite Materials Used for Power and Filters							
Application	Power	Power	Power	Power	Filter	Filter	Filter
Manufacturers	Material Designation						
Magnetics	1* L	2* R	3* P	F	J	W	
Permeability, μ_i	900	2300	2500	3000	5000	10000	
Ferroxcube	3F45	3F3	3C94	3C91	3E27	3E5	3E7
Permeability, μ_i	900	2000	2300	3000	6000	10000	15000
Fair-Rite		77	78		75	76	
Permeability, μ_i		2000	2300		5000	10000	
EPCOS		N97	N72	T41	T65	T38	T46
Permeability, μ_i		2300	2500	2800	5200	10000	15000
TDK Corp.		PC40	PC44	H5A	HP5	H5C2	H5C3
Permeability, μ_i		2300	2400	3300	5000	10000	15000
MMG		F44	F45	F5A	F-10	FTA	FTF
Permeability, μ_i		1800	2000	2300	6000	10000	15000
Ceramic Mag			MN80C	MN8CX	MN60	MN100	
Permeability, μ_i			2050	3100	6500	9000	
TSC Ferrite Int.		TSF-7099	TSF-7070	TSF-8040	TSF-5000	TSF-010K	
Permeability, μ_i		2000	2200	3100	5000	10000	

¹ High Frequency power material 500 kHz & up.
² Lowest loss at 80°C-100°C, 25kHz to 250 kHz.
³ Lowest loss at 60°C-80°C.

Introduction to Molypermalloy Powder Cores

The nickel-iron (Ni-Fe) high permeability magnetic alloys (permalloy) were discovered in 1923 and 1927. Permalloy alloys were successfully used in powder cores, greatly contributing to the carrier wave communications of the time.

In the early 1940's, the Bell Telephone Laboratory and the Western Electric Company developed a new material, trademarked Molybdenum Permalloy Powder (MPP), into cores. This new material was developed for loading coils, filtering coils, and transformers at audio and carrier frequencies in the telephone facility. The use of such cores has been extended to many industrial and military circuits. The stability of permeability and core losses with time, temperature, and flux level, are particularly important to engineers designing tuned circuits and timing circuits. This new material has given reliable and superior performance over all past powder core materials.

Molybdenum permalloy powder, [2 Molybdenum (Mo)-82 Nickel (Ni)-16 Iron (Fe)], is made by grinding hot-rolled and embrittled cast ingots; then, the alloy is insulated and screened to a fineness of 120 mesh for use in audio frequency applications, and 400 mesh for use at high frequencies.

In the power conversion field, the MPP core has made its greatest impact in switching power supplies. The use of MPP cores and power MOSFET transistors has permitted increased frequency, resulting in greater compactness and weight reduction in computer systems. The power supply is the heart of the system. When the power supply is designed correctly, using a moderate temperature rise, the system will last until it becomes obsolete. In these power systems there are switching inductors, smoothing choke coils, common mode filters, input filters, output filters, power transformers, current transformers and pulse transformers. They cannot all be optimally designed using MPP cores. But, in some cases, MPP cores are the only ones that will perform in the available space with the proper temperature rise.

Introduction to Iron Powder Cores

The development of compressed iron powder cores as a magnetic material for inductance coils, stemmed from efforts of Bell Telephone Laboratory engineers to find a substitute for fine iron-wire cores. The use of iron powder cores was suggested by Heaviside in 1887, and again, by Dolezalek in 1900.

The first iron powder cores of commercially valuable properties were described by Buckner Speed, in U.S. Patent No. 1274952, issued in 1918. Buckner Speed and G.W. Elman published a paper in the A.I.E.E.